# Hollow Micro/Nanomaterials with Multilevel Interior Structures

By *Yong Zhao,* and *Lei Jiang**

**In this Review, recent achievements in the multilevel interior-structured hollow 0D and 1D micro/nanomaterials are presented and categorized. The 0D multilevel interior-structured micro/nanomaterials are classified into four main interior structural categories that include a macroporous structure, a core-in-hollow-shell structure, a multishell structure, and a multichamber structure. Correspondingly, 1D tubular micro/nanomaterials are of four analogous structures, which are a segmented structure, a wire-in-tube structure, a multiwalled structure, and a multichannel structure. Because of the small sizes and complex interior structures, some special synthetic strategies that are different from routine hollowing methods, are proposed to produce these interior structures. Compared with the same-sized solid or common hollow counterparts, these fantastic multilevel hollow-structured micro/nanomaterials show a good wealth of outstanding properties that enable them broad applications in catalysis, sensors, Li-ion batteries, microreactors, biomedicines, and many others.**

## 1. Introduction

With the advancement in materials science, considerable research has concentrated on hierarchically complex structured micro/nanometer-scale materials because the microscopic multilevel architectures enable materials a wealth of optimized properties.[1–4] For thousands of years, human beings have known that elemental compositions play an important role in the characteristics of materials like alloys and ceramics. Aided by modern technology in the past few decades, scientists have found that properties of materials can be tuned by downsizing substances to the micro- to nanometer scale instead of changing their chemical compositions. In recent years, it has been further realized that the special micro/nanostructures could also notably influence the performance of materials. As a footing of materials science, various special structured micro/nanomaterials with desired electronic, optical, magnetic, catalytic, and mechanical properties are intensely investigated lately.[1,4]

[*] Prof. L. Jiang, Dr. Y. Zhao
Beijing National Laboratory for Molecular Sciences
Key Laboratory of Organic Solids
Institute of Chemistry
Chinese Academy of Sciences
Beijing, 100190 (P. R. China)
E-mail: jianglei@iccas.ac.cn

**DOI: 10.1002/adma.200803645**

Thanks to the development of modern synthetic technology and analytical instruments, the creation of microscopic materials experienced a structural evolution from simple to complex. In the early days, researchers paid most of their attention to microscopic materials with solid structures such as zero-dimensional (0D) particles or spheres and one-dimensional (1D) rods, wires, or belts as Scheme 1a indicates.[5–12] These materials are regarded as first-generation one-level structures because they are of only a dimensional characteristic. Since the discovery of fullerenes and carbon nanotubes, micro/nanomaterials with a hollow interior such as 0D hollow spheres (or capsules) and 1D tubes (Scheme 1b), became a hot research topic over the past two decades.[4,13–23] In addition to dimensionality, they are of additional hollow interior structure. They could be deemed as second-generation two-level structural micro/nanomaterials. Different to those artificial micro/nanomaterials with complex chemical compositions but relatively simple architectures, nature chose another shrewder route. Derived from a few easily available elements on earth, such as calcium, silicon, and some biomolecules, multilevel micro/nanometer scale building blocks are hierarchically constructed into various biomaterials that exhibit superior mechanical, optical, and many other superior properties.[24–26] In this regard, third-generation micro/nanomaterials with multilevel interior structures, which are of complex interior architectures in addition to dimensionality, have immediately spurred the interest of numerous scientists all over the world in very recent years. This Review is concentrated on the classification, synthesis, and applications of these newly emerging 0D and 1D micro/nanomaterials with unique multilevel interior structures. Generally speaking, we have classified the multilevel interior-structured 0D micro/nanomaterials into four main structural categories, they are a macroporous structure, a core-in-hollow-shell structure, a multishell structure, and a multichamber structure. Correspondingly, 1D micro/nanomaterials also are of four analogous interior structural categories to the 0D objects, which are a segmented structure, a wire-in-tube structure, a multiwalled structure, and a multichannel structure. Scheme 1c shows illustrations of the various mentioned 0D and 1D structures.

Why do we need multilevel interior-structured micro/nanometer-scale objects? An example of a core-in-hollow-shell micro/nanosphere may answer this question from a reflection.

For instance, it is very well known that, in most cases, smaller nanoparticles means higher activities because of the larger specific area.[1,7] A bothersome obstacle, however, exists in that small-sized nanoparticles easily aggregate. Although '1 + 1 = 2' is a universal truth in daily life, this equation is invalid in the nanoworld. The aggregation of nanoparticles will sharply decrease their interface, which inevitably results in the drop of activity. To address this problem, scientists developed a number of countermeasures such as ligand protection and core–shell configuration. Naked nanoparticles, especially various metallic nanoparticles, are extremely unstable and hardly exist. Therefore, they are often decorated with a layer of chemically bonded organic ligands to prevent their aggregation.[11] Nevertheless, such organic ligand nanoparticles are still not stable enough in harsh environments such as at elevated temperature. This is determined by the intrinsic properties of organics. Alternatively, core–shell-structured nanoparticles with an active core and inert shell (like silica or carbon, etc.) are created. Such inorganic composite materials are usually of excellent stability.[27] But in these cases, the core materials are compactly stuck to the shell materials. It may reduce the activity of the core materials to some extent. Core–hollow shell structured micro/nanospheres effectively solve most of these problems.[28] Such novel-structured 0D materials possess a protective hollow shell, in which a freely movable core is enclosed. On the one hand, the solid protective shells could effectively isolate individual core particles and prevent them from aggregating, they thereby provide a relatively homogeneous environment around the wrapped particles' surface. On the other hand, the core particle is freely live in the cavity of the shell, which exposes its active surface sufficiently. It hence exhibits a number of improved properties compared to normal nanomaterials with simple solid or hollow structures. Similarly, other different multilevel-structured micro/nanomaterials also possess their unique predominance than the same sized solid counterparts.

Therefore, these multilevel structural micro/nanomaterials are so attractive not only because of their fantastic interior architectures, but also for a good few more important reasons. Above all, the successful creation of these oddly microscopic objects itself is a proud representative of the advancement of modern synthetic technology.[28–42] It is very helpful to deepen the comprehension of the micro/nanostructural formation mechanism, which will spur inspirations on designing more and more novel structured micro/nanomaterials. Secondly, compared with either bulk or simple micro/nanosized counterparts, the microscopic interior spaces and multiphase interfaces might cause a number of variations in the physicochemical properties. It will reinforce our realization of the micro/nanometer-scale interfacial effects.[31,34,40,42] Finally, the complex interior structures will enable us to better control the local chemical microenvironment that can bring many potential applications.[43–46]

In this Review, along the groupings of Scheme 1c, we will introduce some representative progress towards these micro/nanomaterials with multilevel interior structures. So far as this report is concerned, there are two aspects worthy of note. First, multiwalled carbon nanotubes[47–51] and micro/meso/macroporous zeolites[52–55] are undoubtedly of multilevel interior structures, however, since there have been quite a number of intensive review articles about these two categories of materials, this review would not include them. Second, there are also some micro/nanomaterials of complex epitaxial multilevel

**Yong Zhao** is currently an assistant professor at ICCAS. He received his Ph.D from ICCAS, China in 2007 (with Prof. Lei Jiang). His current scientific interests are focused on the electrostatic force fabrication of multilevel-structured micro/nanomaterials, photocatalysis, and smart multifunctional materials.

**Lei Jiang** is currently a professor at the Institute of Chemistry, Chinese Academy of Sciences (ICCAS), and Dean of the School of Chemistry and Environment, Beijing University of Aeronautics and Astronautics. He received his B.Sc. degree (1987), M.Sc. degree (1990), and Ph.D. degree (1994) from Jilin University of China (Jintie Li's group). He then worked as a postdoctoral fellow in Professor Akira Fujishima's group in Tokyo University. In 1996, he worked as a senior researcher in Kanagawa Academy of Sciences and Technology under Professor Kazuhito Hashimoto. He joined ICCAS as part of the Hundred Talents Program in 1999. His scientific interest is focused on bioinspired surface and interfacial materials.

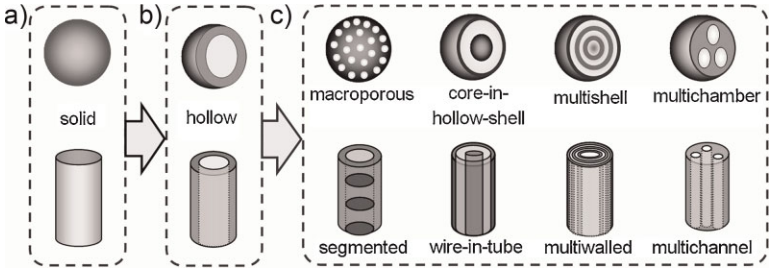


**Scheme 1.** Structural evolution of 0D and 1D micro/nanomaterials. a) First-generation one-level structures with solid interiors: 0D particles and 1D rods and wires. b) Second-generation two-level structures with completely hollow interiors: 0D capsules and hollow spheres, and 1D tubes. c) Third-generation multilevel structures with diverse complex interiors: 0D macroporous spheres, core-in-hollow-shell spheres, multishell spheres, and multichamber spheres, and 1D segmented tubes, wire-in-tube tubes, multiwalled tubes, and multichannel tubes.

structures that include various branched structures such as 0D micro/nanomaterials with rambutan-like (or so-called chestnut-like or urchin-like etc.) structures,[56–59] and 1D micro/nanomaterials with unilateral comb-like, bilateral fishbone-like, and stereoscopic tree-like structures.[58,60–70] These complex structured materials are also very interesting but will not be discussed here because this Review will mainly concentrate on the interior structures. In the following sections, we will first discuss the synthesis of 0D micro/nanomaterials with multilevel interior structures. We will then introduce the preparation of 1D micro/nanomaterials with analogous multilevel interior structures. Some representative applications of these novel materials are then presented. Finally, we will give some personal opinions on the future development of these fantastic micro/nanosized multilevel structural materials.

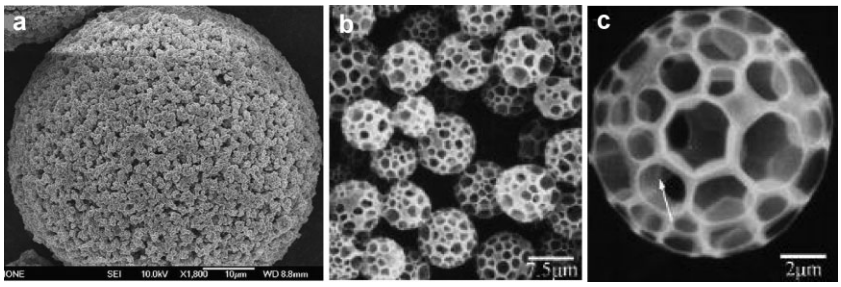


**Figure 1.** SEM images of a) membrane emulsification-generated poly(styrene-divinyl benzene) macroporous microspheres. Reproduced with permission from ref. [82]. Copyright 2007 Sciencedirect. b) and c) PMMA macroporous microsphere emulsion synthesized by using PS colloids as stabilizer. Reproduced with permission from ref. [74]. Copyright 2005 American Chemical Society.

## 2. Multilevel Interior Structured 0D Micro/Nanomaterials

### 2.1. Macroporous Spheres

Macroporous spheres are microspheres saturated with micrometer to submicrometer pores. Although the size of the pores are smaller than the spheres, they are still of a similar order of magnitude. This kind of material can be regarded as a microspherical sponge. Compared with the same sized solid materials, such a macroporous structure greatly enlarges the specific area and economizes raw materials. An effective and popular method to generate macroporous structures is the emulsion route.[71–82] Ma and co-workers have used a microporous membrane emulsion technique to prepare various macroporous microspheres.[79–82] The membrane emulsification technique refers to the introduction of one liquid phase (such as an oil) into another immiscible liquid phase (such as water) through a porous membrane. The oil that passes through the porous membrane will be broken up into microdroplets and then is dispersed into the water to form an oil-in-water (O/W) emulsion. It can generate uniform sized droplets with low energy and low shear. Ma et al. used a Shirasu porous glass (SPG) membrane, which is a special glass membrane with uniform pore size distribution, to generate an O/W emulsion. Because of the hydrophilic properties of SPG and the uniformity of the pore size, the O/W emulsions with uniform-sized oil droplets can be obtained by pressing the oil phase through the pores of the membrane into the aqueous phase that contains a stabilizer and surfactant, under adequate pressure. Because various polymers or biomacromolecules can easily dissolve in the oil phase, this method is readily available to generate organic macroporous microspheres. As an example, Ma et al. prepared poly(styrene–divinyl benzene) macroporous microspheres as shown in Figure 1a by using this membrane emulsification.[82]

Ge and co-workers have synthesized hollow polymer microspheres with a macroporous shell by combining the emulsion method and template method.[74] They first synthesized a kind of surface-sulfonated polystyrene (PS) colloid, which acted as both emulsion stabilizer and pore template. These modified PS colloids were introduced into the water phase of the water–monomer (methyl methacrylate) two phase liquids, and then the PS self-assembly located at the interface of the two liquid phases. After emulsification by stirring, the O/W microemulsions were generated in which the monomer microdroplets were coated with PS colloids. By irradiating the emulsion with $\gamma$-rays, the monomer droplets polymerized and experienced a volume shrinkage process at the same time. This shrinkage crowded out the PS colloids on the interface and left behind cavities on the solidified spheres, in other words, it formed poly(methyl methacrylate) (PMMA) macroporous hollow microspheres (Figs. 1b and 1c). Besides PMMA, other polymeric macroporous spheres could also be fabricated by this method, such as poly(vinyl acetate) (PVA) macroporous spheres. As a branch of the emulsion method, the microfluidic technique has also been explored to fabricate macroporous microspheres. Stone and co-workers proposed a special microfluidic device that could integrate gas–water–oil (three) phases into the microfluidic channels, it thereby generated macroporous polymer microparticles.[71]

Another very accessible approach to form macropores is the spray method. It includes electrospray techniques and the pressure spray drying method. Electrospray is an electrohydrodynamic atomization process in which a high voltage charged conductive liquid flow is broken up into tiny droplets owing to electrostatic repulsion. Electrospray is most commonly used in mass spectrometry for atomization. In addition, this atomization technique is also widely employed to generate micro/nanoparticles. Jiang and co-workers have demonstrated that polymer macroporous microparticles with variable morphologies could be facilely fabricated by electrospray.[83,84] PS was dissolved in *N,N*-dimethylformamide (DMF) to form a homogeneous dilute solution. The solution was then loaded into a syringe with a metallic nozzle. After an appropriate high voltage was applied on the nozzle, the solution was atomized into fine particles and collected on the counter electrode. Figures 2a and 2b show the as-obtained PS particles that are fabricated from 7 and 5 wt-% PS/DMF solutions, respectively. They are of quite different shapes,

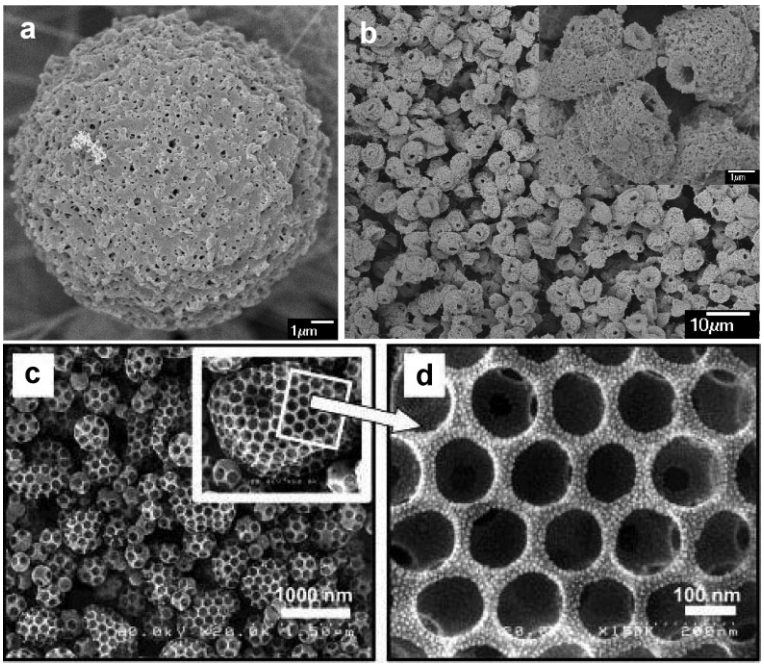


**Figure 2.** Scanning electron microscopy (SEM) images of macroporous 0D materials obtained by spray methods. a) Spherical and b) hollow conical PS macroporous microparticles obtained by electrospray. The formation of pores are induced by microphase separation. Reproduced with permission from ref. [83]. c,d) Silica macroporous microspheres generated by the template stuffed spray drying method. Reproduced with permission from [88]. Copyright 2002 American Chemical Society.

from a spherical to hollow conical shape. It indicates that morphologies of electrospray products could be easily controlled by the concentration of solution. Despite the shape difference, all of these particles possess macroporous structures that are induced by microphase separation effects. When the charged PS/DMF solution was split to tiny droplets, the solvent violently and rapidly evaporated because of the large specific area of the droplets. Such evaporation cooled the droplets to a relatively lower temperature than atmosphere. Thus, the water vapor in air condensed on these cold PS/DMF droplets. Because the PS and water are immiscible, microphase separation occurred on the water-condensed sites and led to the formation of a macroporous structure. Another spray drying method was also successfully applied for the preparation of macroporous microspheres. Okuyama and co-workers have prepared silica and titania macroporous microspheres by template spray drying.[36,85–88] It is often operated by processes that include template filling, figuration, and template removing. Typically, a suspension solution is prepared that is composed of a mixture of framework materials and latex (such as organic PS, PMMA, or inorganic silica) spheres. The suspension is then configured and solidified into microspheres, in which the framework materials are stuffed with latex spheres. After the latex spheres are selectively removed by appropriate physical or chemical approaches, they leave a number of voids. The macroporous microspheres are then obtained. Figures 2c and 2d exhibit the as-prepared silica macroporous microspheres.

In addition, Yan and co-workers have synthesized amphiphilic hyperbranched multiarm copolymers that could form large vesicles by supramolecular self-assembly.[89] They synthesized a poly(3-ethyl-3- oxetanemethanol)-*star*-poly(ethylene glycol) (HBPO-*star*- PEO) hyperbranched multiarm copolymer with a HBPO core and many short PEO arms. The amphiphilic macromolecules could self-assemble into microfoams in water.

### 2.2. Core-in-Hollow-Shell Spheres

Core-in-hollow-shell spheres are structures in which one (or several) movable core particle(s) is enclosed in a hollow micro/nanosphere. The core particle and the outer shell could be either an identical material or two kinds of different materials. They could be regarded as a variation of the ordinary core–shell structure. As for traditional core–shell particles, the core and shell components are compactly attached without any interspaces.[27] The core-in-hollow-shell spheres, however, are of a void intermediate layer. A good number of scientists paid great attention to this interesting structure and denoted them some pictographic names such as the rattle-type[90–93] structure or yolk–shell[94–96] structure. To express this more concisely, we have also referred to the core-in-hollow-shell structures as rattle-structures hereinafter. Consequently, varieties of synthetic approaches have been developed to generate such rattle-structured 0D materials. The template method is probably the most familiar means of synthesis with good reliability and control.[35,44,46,90–92,94,97–107] First, one needs to prefabricate core–shell spheres with two different substances, which serve as both template and core supplier. Second, the core–shell spheres are physically or chemically coated with a layer of the third substance, to thereby form an egg-like composite with a three-layered structure similar to 'yolk, egg white, and eggshell'. When the 'egg white' is selectively removed by an appropriate method (such as chemical etching or calcination), rattle-structured spheres are obtained. Xia and co-workers have proposed a representative approach to fabricate such a hybrid material in which Au nanoparticles are embedded in a hollow poly(benzyl methacrylate) (PBzMA) shell.[104] They first synthesized $Au@SiO_2$ core–shell composite colloids by coating Au nanoparticles with tetraethyl orthosilicate to form an amorphous silica layer. A layer of (chloromethyl)phenylethyltrichlorosilane, an atom transfer radical polymerization initiator, was bonded onto the surface of the $Au@SiO_2$ colloids and reacted with BzMA to form an outer layer of PBzMA. Figure 3a shows the $Au@SiO_2$@PBzMA nanospheres, in which every Au nanoparticle is confined at the center of the individual spheres. After the silica spacer layer was selectively etched by HF solution, Au@PBzMA rattle-structured nanospheres were generated as shown in Figure 3b. It is very clear that the Au nanoparticles are not adhered to the outer shell. The advantage of this method lies in its good controllability: the core sizes, the middle cavities' volume, and the thickness of outer shell are all independently adjustable by tuning the experimental parameters in different reactive procedures.

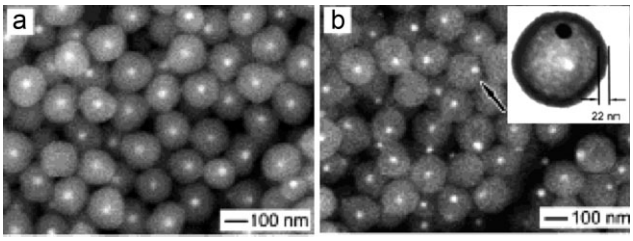


**Figure 3.** Backscattering SEM image of $Au@SiO_2@PBzMA$ particles before (A) and after (B) HF etching. The inset of (B) is the TEM image of Au@PBzMA particles. Reproduced with permission from [104]. Copyright 2003 American Chemical Society.

By using similar strategies, various rattle-structured micro/nanospheres have been created. For example, Arnal and co-workers have also used $Au@SiO_2$ core–shell particles as templates. By coating a layer of $ZrO_2$ and then removing the $SiO_2$, $Au@ZrO_2$ hollow nanospheres are fabricated.[44] Choi and co-workers have fabricated AuPt hybrid particles enclosed in a hematite hollow shell.[100] Still various rattle-structured hollow spheres have been prepared including homogeneous $SiO_2@SiO_2$,[108] or heterogeneous Pt@C,[109] $Au@SiO_2$,[94,102,110] and a good number of others. These rattle-structured spheres mostly show a spherical morphology since they start from spherical templates. The flexibility of the template approach lies in that the ultimate shape of the product is decided by the shape of the initial template. If the template is of an unsymmetrical figuration, the product would also display replicated non-spherical morphologies. For instance, Lou and co-workers have made some remarkable progress on the creation of various non-spherical rattle-structured micro/nanomaterials.[28,35,98,111] They prepared cocoon-like rattle-structured hollow spheres from a spindle $\alpha$-$Fe_2O_3$ template.[35,98,111] The hematite spindles were first coated with a layer of silica to produce the oval hematite@silica core–shell particles. The single- or double-walled polycrystalline $SnO_2$ shell was then deposited on the hematite@silica particles by hydrothermal reaction. After the intermediate $SiO_2$ layer was etched by NaOH or HF, rattle-structured $SnO_2$@hematite hollow cocoons were obtained as shown in Figure 4a and 4b. By tuning the experimental conditions, double-walled rattle $SnO_2$@hematite hollow cocoons could be generated as shown in Figure 4c and 4d. These works have proven that the template method is a programmable and reliable means to generate various rattle-structured objects from a variety of materials. Nevertheless, the utilization of a template determines that this approach needs an inherent multi-step process. In this regards, various more straightforward synthetic strategies have been developed.

For inorganics, several popular crystal hollowing strategies base on such phenomena as the Kirkendall effect and Ostwald ripening mechanism are employed to generate rattle-structured objects. The Kirkendall effect refers to the different atomic diffusive rates between two coupled components. This diffusion difference will generate vacancies in the lower-melting component side of the diffusion couple near the interface. In recent years, scientists found that a nanometer-scale Kirkendall effect could be used to create hollow nanostructures by controlling the atomic diffusion directions and consequential vacancy accumulation. Therefore, this method is widely used to generate hollow nanoparticles or nanotubes.[32,34,112] More interestingly, the rattle-structured nanocrystals are available in the hollowing reaction process. Yin and co-workers have first demonstrated that hollow or rattle-structured nanocrystals could be synthesized by a nanometer-scale Kirkendall effect.[34] As a sample, they introduced an Se suspension into a pre-synthesized Co nanoparticles' solution at 455 K, and then the morphology of the CoSe nanocrystal was tracked by reaction time as shown in Figure 5a. When the Se suspension was injected into the Co nanocrystal solution, the initial solid metallic Co nanocrystal rapidly turned into Co@CoSe hollow structured CoSe nanocrystals. Because of the difference in diffusion rate between Co and CoSe, the Co core gradually diminished and the void between the core and the shell grew simultaneously. After 30 min, the Co core was exhausted and left behind a hollow CoSe nanocrystal. It was revealed that the rattle-structure is an intermediate state of the Kirkendall diffusion, which provided an opportunity to control the inner structures of nanocrystals.

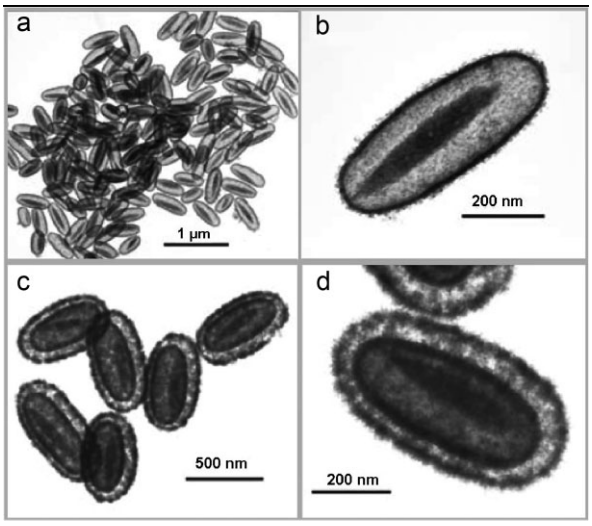


**Figure 4.** TEM images of a) and b) single-walled and c) and d) double-walled $\alpha$-$Fe_2O_3@SnO_2$ non-spherical hollow materials fabricated against a spindle $\alpha$-$Fe_2O_3$ template. Reproduced with permission from [35].

A number of other rattle-structured nanoparticles have also been successfully synthesized by this Kirkendall hollowing effect. Wang and co-workers have prepared a series of organic–inorganic rare earth hybrid rattle-structured particles.[113] They used a one step self-templated synthetic route to generate various structured hybrid rare earth nanomaterials from hollow structured to core–shell structured to rattle structured. Figure 5b and 5c show hybrid yttrium and holmium rattle-structured nanospheres.

Another important solution synthesis strategy towards rattle-structures is based on the Ostwald ripening mechanism.[31,43,99,114–116] Ostwald ripening refers to the solution growth of larger crystals from those of smaller size. This is a thermodynamically driven spontaneous process because a larger crystal is more energetically stable than a smaller one. To lower the total energy of the particles' solution, molecules on the surface of small particles will diffuse and recrystallize on the surface of

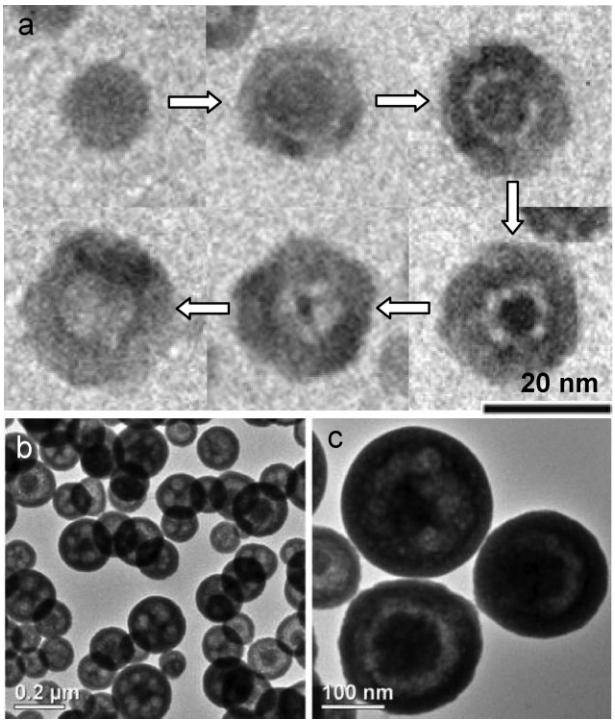


**Figure 5.** a) Kirkendall hollowing evolution process of CoSe nanocrystals as the arrows indicate: from solid particle to rattle-structured particle to ultimate hollow one. Reproduced with permission from [34]. Copyright 2004 American Association for the Advancement of Science. b) Yttrium carboxylate and c) holmium carboxylate rattle-structured nanospheres. Reproduced with permission from [113].

larger particles. As a result, the larger crystals grow and the smaller ones are consumed. Ostwald ripening has been widely used to generate hollow inorganic micro/nanocrystals. Zeng and co-workers have synthesized a series of rattle-structured inorganic semiconductor micro/nanoparticles by Ostwald ripening.[31,115,116] They have demonstrated four instances of Ostwald ripening as exhibited in Figure 6a. They are: 1) a core hollowing process for the preparation of common hollow particles, 2) symmetric Ostwald ripening and 3) asymmetric Ostwald ripening for formation of a homogeneous rattle-structure, and 4) a combination of 1 and 2 to generate multishell particles. The rattle-structured ZnS spheres were synthesized by proposed symmetric Ostwald ripening as shown in Figure 6b and 6c. In this reaction, the tiny ZnS crystallites first aggregated into solid spheres. With prolonged time, the loosely packed crystallites on the outer surface of the particles worked as nucleation points for the recrystallization process. With the formation of a recrystallized shell and, at the same time, the consumation of the underlayer crystallites, a void that surrounded the underneath of the shell formed and divided the sphere into a core and a hollow shell, i.e., a homogeneous rattle-structured ZnS nanosphere (Fig. 6b). If the reaction time was further prolonged, the core was gradually consumed to smaller one, while the void simultaneously became larger (Fig. 6c). This ripening process occurred entirely centrosymmetrically, it thereby formed a concentric rattle structure. As a comparison, Zeng et al. found that some substances could perform ripening in another asymmetric manner. $Co_3O_4$ crystallite aggregates were demonstrated as a model of this asymmetric ripening. Figure 6d shows the asymmetric inner structured $Co_3O_4$ hollow spheres. Zeng et al. attribute the formation of an asymmetric structure to the inhomogeneous distribution of crystallites. It is believed that the hollowing occurred at the domain where the crystallites are smaller and/or less dense. Interestingly, more complex inner structures could also be achieved by the combination of hollowing ripening and symmetric ripening. Figure 6e shows the resultant ZnS hollow spheres with a hollow core, it can be viewed as a double-shelled hollow sphere.

### 2.3. Multishell Spheres

Just as the name implies, multishell spheres are spheres of multiple concentric shells with different diameters. It can be regarded as a nestification of several hollow spheres. Some scientists vividly called them 'onion' structures[117] or 'Russian doll' structures. Partially similar to rattle-structured materials, multishell micro/nanospheres are also often synthesized by a template method and self-assembly approach. Generally speaking, ordinary hollow spheres with a single shell could be generated by coating against a solid spherical template to form a core–shell structured composite sphere. After the template core is removed, a hollow sphere is achieved.[13] Accordingly, it is comprehensible that if the initial template itself is of a hollow structure instead of a solid one, it is possible to create multishell

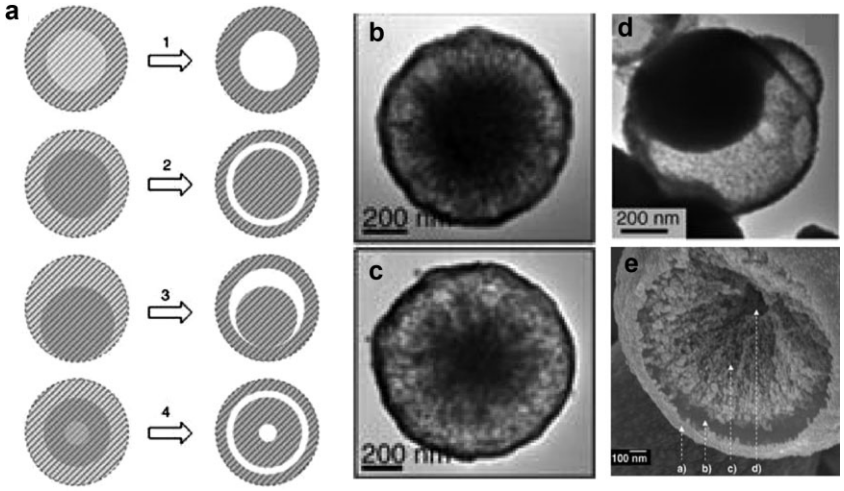


**Figure 6.** a) Schematic illustration of four Ostwald ripening cases: 1) common core hollowing ripening, 2) symmetric ripening, 3) asymmetric ripening, and 4) a combination of cases 1 and 2. Transmission electronmicroscopy (TEM) images of b) and c) rattle-structured ZnS by symmetric Ostwald ripening. d) Rattle-structured $Co_3O_4$ by asymmetric Ostwald ripening. e) SEM image of double-shelled ZnS hollow structure. Reproduced with permission from [116].

hollow spheres by coating the inner and the outer surface of the hollow template, respectively. This method is not complex in concept, but how to practically approach it is not an easy task. On the one hand, suitable hollow spherical templates are not as abundant as common solid template such as PS, $SiO_2$, PMMA, and many other colloids. On the other hand, simultaneous deposition of desired materials onto the outer and inner surfaces, especially the inner surface, of the hollow template to form uniform coatings is not easily controllable. Although it is not so easy, there are still a few multishell microspheres that can be successfully obtained and rely on the template method. Yang and co-workers have employed a kind of special hollow microsphere as template to create double-shelled titania hollow spheres.[30,118] They used a kind of special composite hollow template that was composed of PS hollow spheres that contained a thin hydrophilic inner layer and transverse channels of PMMA–poly(methacrylic acid) (PMA). The hollow sphere template was first treated with sulfuric acid. Such sulphonation of hollow spheres enhances the hydrophilicity of the spheres and provides a suitable graft surface for the subsequent titania coating process. The dry sulfonated hollow spheres were immersed into a $Ti(OBu)_4$ sol to coat a titania layer onto both the inner and outer interface of the hollow spheres. The titania@PS@titania composite multishell hollow spheres were obtained as shown in Figure 7a. If the intermediate PS layer was selectively removed by a suitable solvent, double-shelled titania hollow spheres were prepared as shown in the inset of Figure 7a. The suitable template composition and sulphonation of the template surfaces played important roles in the successful preparation of double-shelled hollow spheres. Use of a composite instead of homogeneous PS hollow spherical template in the experiments is of note. The existence of PMMA–PMA transverse channels on the PS shell act as the entrance for the titania sol. The deposition and the thickness of the titania and intermediate layer are decided by sulfonation time because a higher sulfonation degree results in a thicker titania layer. The template sulphonation time used for the spheres in Figure 7b was longer than that for Figure 7a, it thereby resulted in an increase of the sphere's diameter and a decrease of intermediate layer's distance.

In addition to the utilization of a hollow spherical template, researchers have also used a normal solid template to manufacture multishell spheres indirectly.[117,119–121] It is often performed by a multistep layer-by-layer (LbL) self-assembly process. The surface of the solid template is first decorated with layers of a desired coating by an alternate LbL assembly of a cationic polyelectrolyte and an anionic polyelectrolyte. A second layer of another substance is then coated that can act as an intermediate layer. By further coating a third layer of material onto the second layer, a multilayered core–shell sphere is generated. If the core and intermediate layer is removed, respectively, a multishell hollow sphere is obtained.[122–126] In some cases, the multishell structure and rattle structure are combined when a solid core is wrapped in multiple hollow shells, as indicated in Figure 4c and 4d.[127]

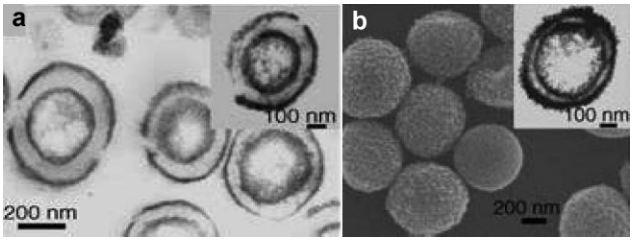


**Figure 7.** a) TEM image of double-shelled titania hollow spheres. b) SEM and TEM (inset) images of titania composite hollow spheres with thicker layers. Reproduced with permission from [30].

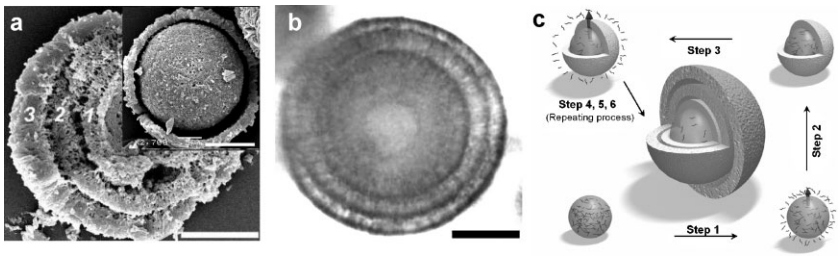


**Figure 8.** a) SEM image of a hollow microsphere with three shells, the inset discloses the hollow intermediate layer. b) Optical microscopy image of the microsphere. c) Schematic illustration of the spatially periodic precipitation mechanism of the layer construction process. Scale bars of (a) and (b) are 10 μm. Reproduced with permission from [128].

Recently, Chen and co-workers prepared multishell microspheres from azithromycin, an amphiphilic pharmaceutical molecule, by using a very simple self-assembly approach.[128] The azithromycin was first dissolved in ethanol to form a homogeneous solution. The solution was slowly added into deionized water under magnetic stirring. The mixed solution rapidly transformed from clear to opalescent. After stirring was stopped and the static solution was stored for several minutes, multishell azithromycin microspheres were obtained. The shell layers could be facilely adjusted by changing the starting concentration of the ethanol solution of azithromycin. Figure 8a and 8b show the self-assembled three-shell hollow microspheres. They are proposed to form by a spatially periodic precipitation process as indicated in Figure 8c.

Azithromycin is a kind of amphiphilic molecule that is soluble in ethanol but insoluble in water. When the ethanol solution of azithromycin is introduced to water, it first forms a suspension of numerous giant vesicles. The azithromycin molecules then diffuse outward with the ethanol because of a concentration gradient of the azithromycin solution from the inside of the vesicle to outside in the bulk solution. The region near the surface of the vesicle may gain a higher concentration of azithromycin molecules (step 1 of Fig. 8c). Since azithromycin is poorly soluble in mixtures with a high proportion of water, the azithromycin will precipitate (step 2 of Fig. 8c) to form the first layer. The precipitation of the first layer results in a local lack of free azithromycin molecules. Therefore, the precipitation process is temporarily terminated and a hollow intermediate layer formed. In succession, azithromycin molecules enveloped within the microsphere still diffuse outward driven by the concentration gradient (step 3 of Fig. 8c). It thereby induces another precipitation stage (step 4 of Fig. 8c). The cycle repeats itself

until the concentration of azithromycin molecules is insufficient for shell precipitation. Therefore, the initial concentration of azithromycin plays an important role in the shell formation. Based on this understanding, multishell microspheres with controllable shell number are available. Still other self-assembly or self-aggregation strategies that have been successfully applied to generate multishell spheres.

### 2.4. Multichamber Spheres

Multichamber spheres are spheres of multiple evenly distributed independent chambers. These chambers are isolated from each other and the outer environment simultaneously. Reports about such materials are relatively few. The main difficulty is how to precisely control the number of inner chambers. Both a template method and crystallography growth route, which are the most thriving methods to produce micro/nanometer-scaled materials with other complicated interior structures, do not easily generate such multichamber structures. From the viewpoint of a template route, the chambers should be the voids of the removed template. Nevertheless, how to wrap a specified number of templates into a sphere and keep them separate are not simple tasks. The crystallography route has shown good feasibility to synthesize inorganic multishell spheres or rattle-structured spheres through the mentioned Ostwald ripening or Kirkendall effect. These phenomena are not, however, very suitable to generate multiple chambers of a desired number because the eccentric voids are energetically unfavorable in the crystallization process. Therefore, such multichamber spheres are seldom obtained by routine synthetic approaches. Few works about this structure are derived from a microfluidic technique that could generated double (or multiple) emulsions through specially designed microfluidic devices. By using a cross junction microchannel integrated with a T-junction microchannel, Torii and co-workers have produced water-in-oil-in-water (W/O/W) or oil-in-water-in-oil (O/W/O) double emulsions in which several tiny droplets with different compositions are independent wrapped in an inverse liquid phase drop.[38,129] Recently, Weitz and co-workers have proposed a novel microfluidic device that is composed of multiple coaxial co-flow microcapillaries.[130] It could produce highly controllable multiple emulsions with very complicated W/O/W/O or O/W/O/W structures. It is worth mentioning that the as-fabricated multiple emulsions should be merely regarded as quasi multichamber spheres because most of them are liquid-in-liquid metastable systems.

Recently, Zhao and co-workers proposed a novel multifluidic compound-jet electrospray technique that could generate multichamber microspheres with adjustable chamber number.[131] The fabrication set-up is sketched in Figure 9a. Several metallic capillaries were embedded separately into a blunt metal needle to form a hierarchical compound nozzle, which was connected with a high voltage generator. A viscous shell fluid was fed to the outer needle at an appropriate flow rate, and several kinds of viscous core fluids were controllably delivered to the inner capillaries, respectively. The core fluids were immiscible or poorly miscible with the shell fluid, so they formed a compound but not mixed pendent drop under the exit of the nozzle. Under a suitable electric field, the compound fluid broke into a spray of charged droplets because of the electrohydrodynamic effect. These droplets solidified into spherical fine particles on the counter electrode. The as-obtained microspheres were of several inner chambers that corresponded to the number of inner fluids. For example, by using two inner fluids, two-chamber microspheres could be generated as shown in Figure 9b. Similarly, microspheres with a chamber number from one to four, which are showed in Figure 9c to 9f, respectively, were also facilely available by simply tuning the configuration of the inner capillaries. It validates the capability and handleability of this versatile technique. Moreover, this technique was also applicable to create multicomponent microcapsules if the inner capillaries were fed into different substances.

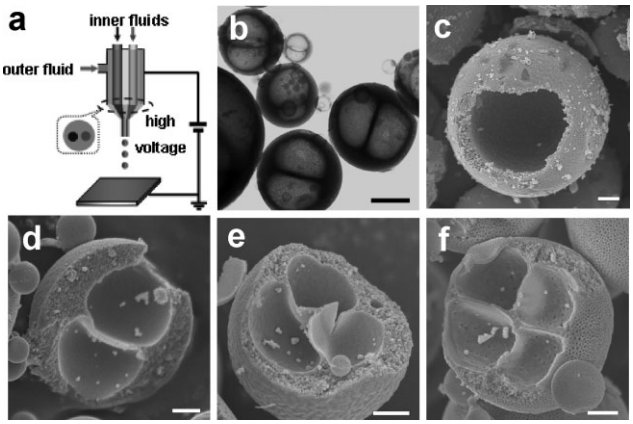


**Figure 9.** a) Multifluidic compound-jet electrospray set-up (here is a device of the generation of two-chamber microspheres). b) TEM image of two-chamber microspheres. SEM of: c) one-, d) two-, e) three-, and f) four-chamber microspheres. Scale bar is 1 μm for (b), and 500 nm for (c–f). Reproduced with permission from [131]. Copyright 2008 American Chemical Society.

## 3. Multilevel Interior Structured 1D Micro/Nanomaterials

These 1D materials could be regarded as the analogs of the above-mentioned 0D materials. For example, 0D macroporous spheres, rattle-structured spheres, multishell spheres, and multichamber spheres correspond to 1D segmented tubes, wire-in-tubes, multiwalled tubes, and multichannel tubes, respectively. Compared with diverse 0D complicated interior architectures, reports on 1D micro/nanomaterials with multilevel interior structures are relatively few. This is probably because the creation of anisotropic 1D microscopic materials with complex interior structures is, to some extent, not as facile as for isotropic spherical 0D materials. Despite this, some 1D multilevel architectural micro/nanomaterials have been successfully created by many ingenious approaches.

### 3.1. Segmented Tubes

Segmented tubes are a type of tubular microscopic material characterized by a micro/nanotube periodically stuffed with

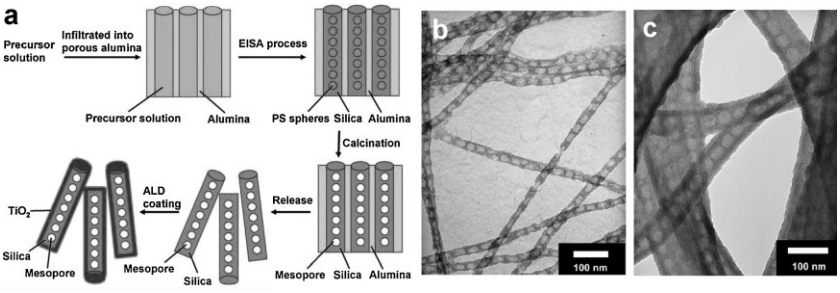


**Figure 10.** a) Scheme of the fabrication of silica and titania/silica hybrid segmented nanotubes. A silica precursor that contained PS-*b*-PEO is filled into a AAO template. The evaporation of the solvent leads to the formation of spherical PS domains evenly dispersed in a silica/PEO continuous phase. After calcination and template removal, segmented silica nanotubes (b) are obtained. It can be further transformed to titania/silica hybrid nanotubes (c) by ALD of a layer of titania on the segmented silica nanotubes. Reproduced with permission from [29]. Copyright 2007 Wiley-VCH.

another substance, which could be either air or some other material such as metals, oxides, and polymers. Some of them are very like a miniaturized bamboo stem. It is well-known that negative anodic nanochannels such as aluminum oxide (AAO) and positive nanowires are often employed as hard templates to prepare 1D tubular materials. These templates are also used to generate segmented tubes. Chen et al. have fabricated bamboo-like titania/silica hybrid nanotubes, what they called 'nanowires that contain linear mesocage arrays'.[29] They used a step-by-step hierarchical templating method that is shown in Figure 10a.

First, they prepared a homogeneous precursor solution that dissolved PS-*b*-PEO, tetraethyl orthosilicate (TEOS), HCl in ethanol, and toluene. Here, the PS-*b*-PEO served as soft templates to subsequently form mesopores. Second, the solution was introduced into an AAO hard template. Upon evaporation of the solvents, microphase separation and gelation occurred in the AAO pores and the hydrophobic PS blocks regularly dispersed in the hydrophilic PEO-TEOS phase. Third, the organic-phase soft template was removed by calcination and then the AAO hard template is etched by acid. Segmented silica nanotubes were then obtained as shown in Figure 10b. The achievement of segmented tubular structures is a result of the combination of a hard template with a soft template. The AAO hard template confinement contributes to the linear tubular structure, while the microphase separation of the PS-*b*-PEO soft template results in the segmented structure. If another substance is deposited on the as-prepared segmented silica nanotubes, it will form hybrid segmented nanotubes. Chen and Steinhart et al. achieved this concept by coating an additive titania layer on silica by atomic layer deposition (ALD).[29] The ALD technique is a reliable method to generate nanometer-scale thin films or overlayers with good conformality and process controllability.[132] Figure 10c shows the as-generated titania/silica hybrid segmented tubes.

Segmented nanotubes can also be obtained by directly using existing nanotubes as a precursor. Owing to the intrinsic hollow properties of carbon nanotubes (CNTs), Yarin and co-workers found that a low-molecular-weight polymer solution could enter into CNTs and form segmented or foamed inner structures.[133] They utilized a kind of open-ended wettable CNT as target. When the CNTs were immersed in a dilute solution of low-molecular-weight polymer, the polymer will enter into the CNTs and concentrate in the CNTs driven by a self-sustained diffusion mechanism. As a result, a series of CNTs with peapod-like (Fig. 11a), foam-like (Fig. 11b), or bamboo-like (Fig. 11c and 11d) structures are achieved.

Rayleigh instability is a common phenomenon in fluid physics. It refers to the instability of a liquid column that will turn to an array of liquid drops in order to lower its total surface energy. This concept was also used to generate segmented nanotubes very recently.[42,134,135] As a result of the route similarity, this method is incorporated into the discussion in the following wire-in-tube section.

### 3.2. Wire-in-Tube

The wire-in-tube micro/nanomaterial is a combination of two kinds of basic 1D architectures, i.e., solid wires and hollow tubes. The architecture is such that a slim wire is embedded parallel into a thicker tube. Just like the mentioned 0D rattle-structured materials are different from the core–shell spheres, this wire-in-tube structure is also different to the core–shell nanowires because there are voids left between the inner wire and the outer tube wall. Unlike the relatively abundant rattle-structured 0D materials, research on such wire-in-tube 1D materials are relatively few.[42,136–138] Knez and co-workers have reported the

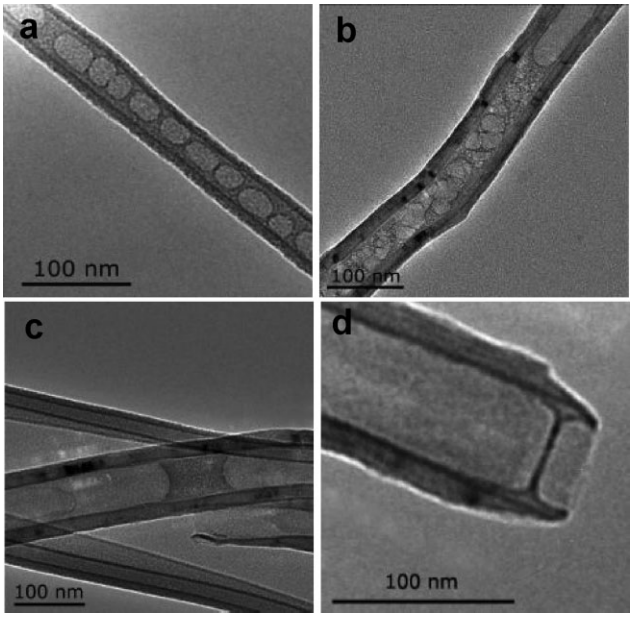


**Figure 11.** PEO deposits inside CNTs that were obtained by dispersing dilute PEO of different molecular-weight in water over dry CNTs. a) Segmented and b) dispersed bubble-structured CNTs from low-molecular-weight PEO (600 kDa). c) and d) Segmented CNTs from high-molecular-weight PEO (2000 kDa). Reproduced with permission from [133]. Copyright 2007 American Chemical Society.

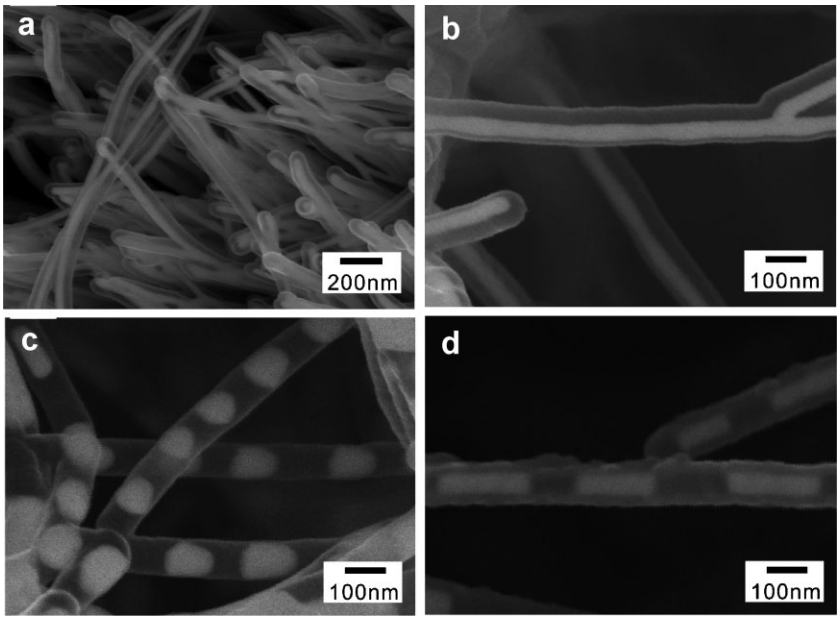


**Figure 12.** a) and b) Au nanowires embedded in $TiO_2$ nanotubes. c) Au nanoparticle chain and d) Au nanorod chain embedded in $TiO_2$ nanotubes after the wire@tube is annealed. Reproduced with permission from [42]. Copyright 2008 American Chemical Society.

fabrication of wire-in-tube nanomaterials by combining ALD with template methods.[42]

As a demonstration, Au nanowires were first prepared by a template method. Second, Au wires were coated with a sacrificial $Al_2O_3$ layer and then with a shell layer of another material (here $TiO_2$) by ALD. It thus formed a $Au@Al_2O_3@TiO_2$ sandwich core–shell nanowire. Third, the $Al_2O_3$ layer was removed and a $TiO_2$ nanotube formed in which a Au nanowire was preserved. Figure 12a and 12b show the $Au@TiO_2$ wire-in-tube nanomaterials. If the $Au@TiO_2$ tube was annealed above the melting point of the Au nanowire, the large surface tension of melted liquid metallic Au nanowire would break up to form a chain of liquid Au nanodroplets because of the Rayleigh instability. These melted metallic nanodroplets freeze into a periodic nanoparticle chain (Fig. 12c) if there is enough inner space in the $TiO_2$ nanotube. Alternately, if the nanotube's inner space is limited, a periodic nanorod chain (Fig. 12d) would form. The morphology of the metallic nanowire formed is determined by the inner space volume of the nanotube. It was calculated that if the inner diameter of the nanotubes is over 3.78 times that of the diameter of the nanowires, the wires will break up into spherical nanoparticles. Otherwise, if this ratio is less than 3.78, the wires will turn into nanorods. The smaller ratio will result in the longer nanorods. This indicates that the inner morphologies of the tubes can be tuned by the variation of initial thickness of the sacrificial $Al_2O_3$ layer.

Zussman et al. have employed a co-electrospinning method to produce polyacrylonitrile (PAN)/PMMA wire@tube microtubes.[136] Electrospinning is a versatile technique to generate ultrafine fibers from a good wealth of materials that has flourished in the last decade.[139–141] Typically, a suitable polymer solution, that flows out through a conductive metallic capillary linked with a high-voltage generator, can be stretched into micro/nanofibers under electrostatic force. Co-electrospinning (also called coaxial electrospinning) modified the routine single spinning nozzle into a coaxial nozzle, which could generate a stream of core–shell compound fluids. It can be used to generate core–shell or hollow fibers.[142,143] Zussman et al. used a PAN/DMF solution as a shell fluid and a PMMA/DMF-acetone solution as a core fluid for co-electrospinning. Owing to the immiscibility of PAN and acetone, the PAN shell undergoes phase separation rapidly at the interface of the PAN and PMMA solution, while the core PMMA solution incompletely solidifies. The subsequent solvent evaporation of the core solution results in the further volume shrinkage of PMMA, the diameter of which is smaller than the inner diameter of the outer PAN tube. It thereby forms PMMA/PAN wire@tube microtubes.

### 3.3. Multiwalled Tubes

Multiwalled tubes are microscopic tubes with several walls just like the well-known multiwalled carbon nanotubes. Xia and co-workers have used a galvanic replacement reaction to prepare Au/Ag alloy multiwalled nanotubes.[18,40,144] They first synthesized Ag nanowires by a polyol process, which then acted as a template and reductant (inset of Fig. 13a). When an aqueous $HAuCl_4$ solution was added into the Ag nanowires, the galvanic replacement reaction started and the $Au^{3+}$ ions were reduced into Au atoms. These Au atoms nucleated and grew into a shell around the Ag templates. The thickness of the Au shell increased along with the consumption of the Ag template. As a result, hollow Au nanotubes were obtained, as shown in Figure 13a, after the Ag nanowires were completely consumed. If the as-prepared Au nanotubes were further electroless deposited with another layer of Ag and the galvanic replacement reaction with $HAuCl_4$ repeated, double-walled Au nanotubes could be created (Fig. 13b). This method provided a relatively versatile route to generate nanotubes or multiwalled nanotubes from a suitable reactive couple. Jiang and co-workers have reported that ZnO nanotubes could be generated by a solution aging route.[59] First, the hexagonal Wurtzite ZnO nanorods were obtained in the reactive solution as shown in Figure 13c. If the reactive system is aged for a longer time, the nanorods would transform to ZnO nanotubes (Fig. 13d) because of a thermodynamically driven process. The non-polar faces of wurtzite ZnO are stable planes, while the polar (001) and (00–1) ones are metastable. During the ZnO nanorod aging process, they tended to reach their thermodynamic stability. Thus the hollowing of the nanorods occurred by preferential chemical solvation of the metastable polar faces and led to the single crystal ZnO nanotubes. This thermodynamic hollowing route is also applicable to produce multiwalled tubes, as has been demonstrated by Yan and co-workers very recently.[145] They have synthesized single-crystalline hematite double-walled nanotubes by a one-step hydrothermal method. In this reaction, solid

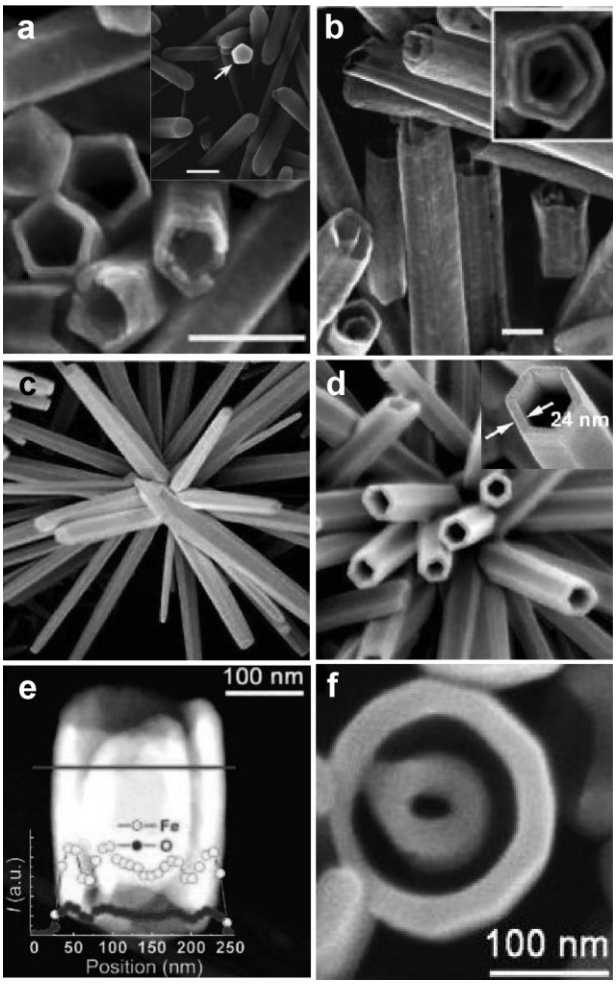


**Figure 13.** a) Single-walled Au nanotubes generated by reducing $HAuCl_4$ with pentagonal Ag nanowires as template (inset). b) After electroless plating a layer of Ag on the Au nanotubes and then performing the galvanic replacement reaction again, double-walled Au nanotubes are obtained. Scale bars: 100 nm. Reproduced with permission from [40]. c) Hollowing of ZnO nanorods to d) nanotubes. Reproduced with permission from [59]. Copyright 2006 American Scientific Publishers. e) and f) The double-walled hematite nanotubes obtained by a one-step hydrothermal reaction. Reproduced with permission from [145]. Copyright 2008 American Chemical Society.

ellipsoid hematite nanocrystals were first obtained. The hollowing occurred not only at the centered tips of the ellipsoid nanocrystals, but also at several high-energy sites on the top simultaneously. These neighboring holes gradually merged into a continuous void upon increasing the reaction time, thus tube-in-tube nanostructures were formed as shown in Figure 13e and 13f.

The self-assembly method is another popular route to prepare multiwalled tubes. Yan et al. have demonstrated that multiwalled tubes can be generated by supramolecular self-assembly.[41] It is derived from a special designed amphiphilic hyperbranched multi-arm copolymer poly(3-ethyl-3-oxetanemethanol) (HBPO)-*star*-PEO with a hydrophobic hyperbranched HBPO core and many hydrophilic PEO arms as illustrated in Figure 14a. When the dried viscous HBPO-*star*-PEO was directly added to acetone under stirring at room temperature, multiwalled tubes were obtained at the surface of acetone as Figure 14b shows. The self-assembly of the hyperbranched multi-arm copolymer is induced by microphase separation and formation of hydrogen bonds. When the hyperbranched copolymer was added to acetone, the hydrophobic interaction of the HBPO cores of the copolymers leads to a spinodal microphase separation and the HBPO cores aggregate in acetone. This process is accompanied by the spontaneous segregation of the HBPO cores and PEO arms. The aggregated hydrophilic PEO arms extend out from the interfaces between the cores and arms because of the repulsion among the arms. With the segregation of HBPO cores and PEO arms, the distance between hydroxy and ether groups or among hydroxy groups in both arms and cores decreases and facilitates the formation of hydrogen bonds. Hydrogen bonds in both the core and arm lamellae can further drive the molecular self-assembly process and strengthen the self-assembly tubes. Finally, the macroscopic tubes with a lamella wall are formed.

In addition, Aida and co-workers have synthesized photoconductive double-walled nanotubes from a trinitrofluorenone-appended gemini-shaped amphiphilic hexabenzocoronene by controlled self-assembly.[146] By hierarchical supramolecular self-assembly of a small organic non-amphiphilic molecule, *para*-terphenylen-1,4″-ylenebis(dodecanamide), Bo and co-workers prepared rolled-up multiwalled nanotubes.[147] Other multiwalled tubular materials including polymer tubes by wetting of the AAO template[148] and by a self-rolling method,[149] $Cu_7S_4$ by a sacrificial templates method,[150] and some others.[51,148,151–157]

### 3.4. Multichannel Tubes

Multichannel tubes refer to 1D objects with multiple independently parallel hollow channels, which are somewhat like a bundle of single-walled tubes. Many natural creatures are of such multichannel microstructures such as lotus roots and some bird's feathers. Scientists have also demonstrated that a multichannel structure could be used for DNA transport[158] and solar cells.[159] Unfortunately, the literature about artificial 1D multichannel micro/nanomaterials is extremely rare. Lately, Jiang and co-workers have proposed a powerful multifluidic electrospinning technique that could fabricate multichannel micro/nanotubes with a programmable channel number.[39] The experimental set-up of the multifluidic compound-jet electrospinning is somewhat similar to the above-mentioned multifluidic electrospray devices. Two kinds of immiscible viscous liquids served as shell and core fluids that were fed into the outer nozzle and several inner capillaries separately. It is noted that the outer fluids should be a kind of good spinnable solution. After an electrospinning process, a fibrous film was collected on the counter electrode. By removing the organics of the as-prepared products through calcination, multichannel microtubes were obtained.

Figure 15a is the scanning electron microscopy (SEM) image of the cross section of a $TiO_2$ three-channel microtube, which is obtained by using a poly(*N*-vinyl-2-pyrrolidone) (PVP)/Ti(*i*OPr)$_4$ sol as the outer solution and paraffin as the inner fluidic system. Figure 15d shows the three channels more clearly and how the

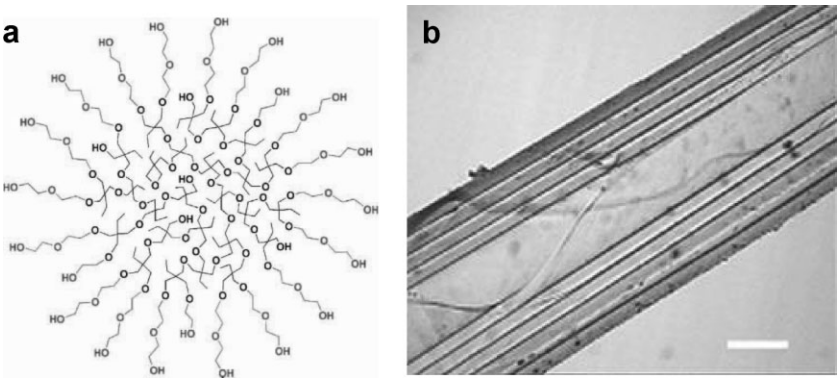


**Figure 14.** a) Diagrammatic sketch of the HBPO-*star*-PEO multi-arm copolymer with HBPO core and PEO arms. b) Optical microscopic image of the pentawalled self-assembly microtubes in acetone. Scale bar: 300 μm. Reproduced with permission from [41]. Copyright 2004 American Association for the Advancement of Science.

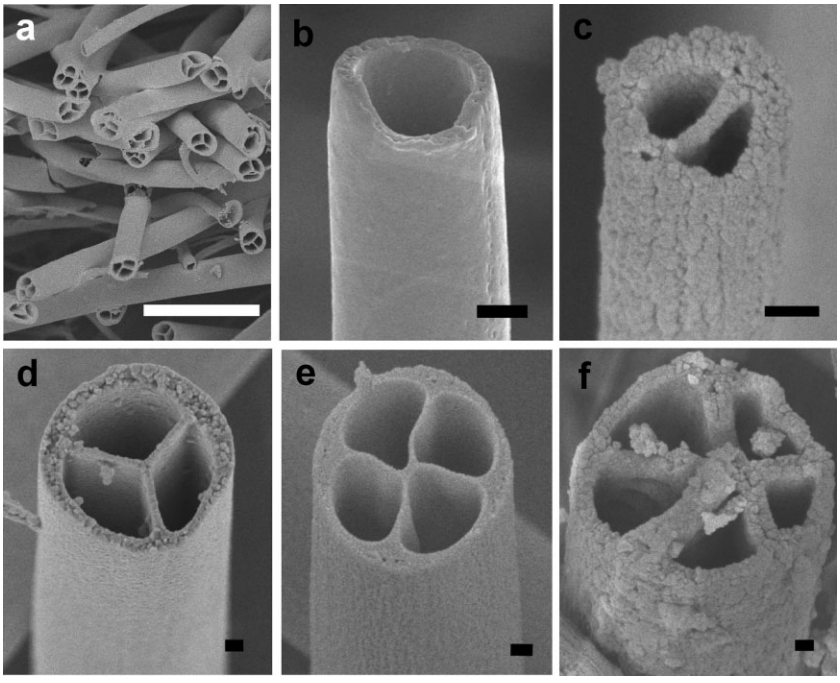


**Figure 15.** a) SEM image of large-area titania three-channel microtubes. b–f) SEM images of multichannel tubes with a channel number from one to five. The scale bars are 10 μm for (a) and 100 nm for (b–f). Reproduced with permission from ref. [39]. Copyright 2007 American Chemical Society.

trifurcate ridge embeds in the tube shell and partitions the tube into three flabellate parts. The predominant advantages of this approach lies in that the composition, wall thickness, and tube diameters are all facilely controllable by simply adjusting the relative experimental parameters. Moreover, the channel number can also be tuned by changing the configuration of the compound nozzle. Figures 15b–15f demonstrate fabricated microtubes with channel numbers from 1–5 that are derived from compound nozzles with same number of inner capillaries, respectively. It validates the good fidelity and effectiveness of this multifluidic compound-jet electrospinning technique.

## 4. Applications

The attraction of hollow micro/nanomaterials with multilevel interior structures lies in their large number of predominant properties, which include high specific areas, abundant inner voids, multiphase heterogeneous interfaces, and many others. In many cases, these characteristics make them superior to either bulk materials or the same sized materials with simple structures. They are thereby competitive in many important areas, here we merely present a few representative applications in catalysis, sensors, Li-ion batteries, drug-delivery, microreactors, and biomedicines.

### 4.1. Catalysis

Thanks to the huge specific area and multiphase heterogeneous interfaces, the most straightforward applications of multilevel interior structured micro/nanomaterials are in catalysis. As a typical example, Okuyama and co-workers have fabricated macroporous brookite $TiO_2$ microspheres by spray drying a $TiO_2$ nanoparticle suspension with a PS latex template, which exhibited improved photocatalytical properties than the same sized solid counterparts.[85] First, a suspension was prepared by mixing brookite titania nanoparticles with the PS latex template. The composite suspension was then sprayed into a two-zone furnace. It broke up into aerosol microdroplets and then dried to $TiO_2$/PS hybrid microspheres immediately at the first low-temperature zone (200 °C). After the hybrid microspheres were blown into the second high-temperature zone at 500 °C, the organic PS spheres were removed that left submicrometer cavities in the $TiO_2$ microparticles, i.e., macroporous $TiO_2$ microparticles. By changing the size and concentration of the PS latex template, $TiO_2$ microspheres with tunable porosity could be obtained. Compared with pure $TiO_2$ nanoparticles, Okuyama and co-workers found that microparticles with a proper porosity exhibit relatively equivalent photocatalysis properties. Furthermore, the macroporous microparticles have an obviously enhanced photocatalytic activity compared to dense microparticles of the same size. This is mainly a result of the increased specific area, which is favorable for the titania photon absorption. Although the phocatalytic performance of macroporous $TiO_2$ particles has not exceeded the nanoparticles, they still possess considerable advantages compared to normal nanoparticles. As is known, the large problem of nanoparticle utilization lies in the very troublesome and expensive downstream nanoparticle removal processes. Macroporous structured microparticles can solve the problem in that

they are easier to collect and reuse. This may provide inspirations for many other catalytic systems.

The improved catalytic abilities of macroporous materials are mainly achieved by increasing their specific areas. More importantly, the rattle-structured or multishell micro/nanoparticles exhibit highly efficient catalytic properties not only because of the large specific area, but also because of their unique hollow shell, which effectively stabilizes the active core. The tiny inner cavity between the hollow shell and the core particle implies huge opportunities for a wealth of catalytic applicable areas. Ikeda and co-workers have reported that platinum nanoparticles embedded in hollow porous carbon shell (Pt@C) rattle-structured nanoparticles are of high activity as a heterogeneous hydrogenation catalyst.[109] The Pt@C nanoparticles were fabricated through a sequential coating process. First, PVP-stabilized Pt nanoparticles were synthesized. Second, a silica layer and mesoporous silica layer was deposited on the Pt nanoparticles (Pt@$SiO_2$-*m*$SiO_2$). Third, a layer of carbon was cast onto the mesoporous silica layer to form Pt@$SiO_2$-*m*$SiO_2$-C composite nanoparticles. After the silica was etched by HF solution, rattle-structured Pt@C nanoparticles were obtained as shown in Figure 16a. To characterize the catalytic ability of Pt@C nanoparticles, a nitrobenzene hydrogenation reaction was conducted by comparing with several other kinds of Pt catalysts, which were intermediate products of the above-mentioned rattle-structured Pt@C nanoparticles, i.e., Pt-PVP nanoparticles, Pt@$SiO_2$-*m*$SiO_2$, and another commercial Pt catalysts supported on activated carbon (Pt/AC). Figure 16b gives the comparative results of these Pt catalysts. The Pt@C nanoparticles had evident superiority over the other Pt catalysts in that almost all the nitrobenzene was catalyzed into aniline. Moreover, the rattle-structured Pt@C could be easily recovered and reutilized without activity reduction.

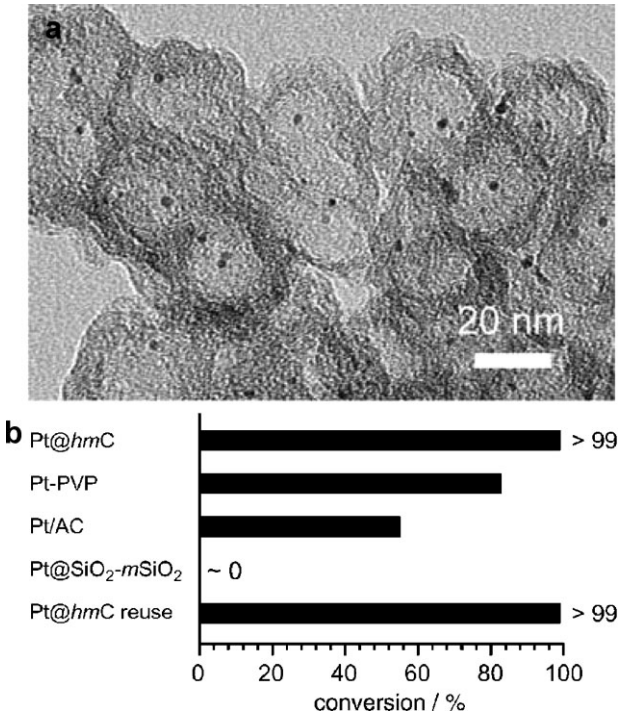


**Figure 16.** a) Rattle-structured Pt@C hollow nanoparticles. b) Catalytic hydrogenation activity of nitrobenzene into aniline of various structured Pt. The rattle-structure possesses the leading performance even after it is reused. Reproduced with permission from ref. [109].

### 4.2. Sensors

Zhu and co-workers have synthesized multishell hollow $Cu_2O$ microspheres that show improved sensitivity to ethanol gas.[43] They were synthesized by a solvothermal reaction from $Cu(NO_3)_2 \cdot 3H_2O$ and glutamic acid in ethanol. The $Cu_2O$ microspheres are shown in Figure 17a, and are evidently multiple hollow shells. The formation of multiple shells is attributed to the Ostwald ripening mechanism. The sensitivity of the multishell hollow $Cu_2O$ microspheres was measured towards 100 ppm ethanol. Compared with similar sized solid $Cu_2O$ microspheres, the sensitivity of the multishell $Cu_2O$ microspheres was evidently improved from 1.5 to 8.2 as indicated in Figures 17d and 17b. To evaluate the nanosize effect on the sensitivity, the multishell hollow $Cu_2O$ microspheres were crushed into nanoparticles. Although the nanosized $Cu_2O$ showed a better sensitivity of 2.7 than solid microspheres (Fig. 17c), it is still much less than the multishell hollow microspheres. These results indicate that, although the nanocrystals could increase the sensitivity because of the higher specific area, the relatively close stacking limited the advantage of small size effect because the analyte gas molecules could only access a thin surface layer of the sensing substances. Comparatively, the multishell $Cu_2O$ microsphere sensors possess a greater

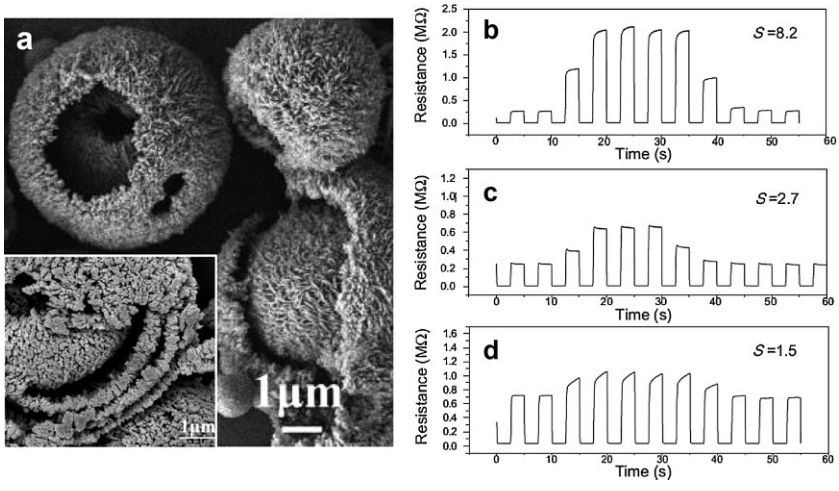


**Figure 17.** a) SEM image of multishell $Cu_2O$ hollow spheres. Dynamical responses to 100 ppm ethanol gas of the $Cu_2O$ sensor with: b) multishell hollow microspheres, c) nanocrystallites, and d) solid microspheres with an average diameter of 500 nm. Reproduced with permission from ref. [43].

surface accessibility which contributes to the higher sensitivity. It means the multishell structure plays an important role in the improvement of the sensitivity.

### 4.3. Li-ion Batteries

Lithium-ion batteries (LIBs) are a hot research topic in both scientific and industrial domains nowadays. One of the most important issues surrounding LIBs is the production of appropriate electrode materials that make for a higher energy density and more cycle characteristics. A good few unique rattle-structured hollow materials have been verified to be good candidates for LIB by many researchers.[46,98,99,160–162] Wan and co-workers have synthesized tin nanoparticle-encapsulated elastic hollow carbon spheres (TNHCs) rattle-structured nanomaterials that worked as anode materials. They exhibited improved performances in LIBs.[46] Compared with graphite, a traditional anode material, metallic tin is of higher specific capacity, higher operating voltage, and has no solvent intercalation. However, the huge volume change during the Li–Sn alloying–dealloying process limits its practical applications as an anode material. Wan et al. ingeniously solved this problem by enclosing the Sn nanoparticles into hollow carbon shells. The void space of the carbon hollow shell provides enough tolerance for the volume variation during the $Li^+$ insertion/extraction cycle. The TNHCs electrode materials were synthesized as follows. First, a layer of $SnO_2$ was deposited onto the spherical silica template by hydrolysis of $Na_2SnO_3$ under hydrothermal conditions. The silica was then etched by NaOH to leave a $SnO_2$ hollow sphere. Afterwards, a layer of carbon was coated onto the $SnO_2$ hollow sphere by pyrolysis of glucose under secondary hydrothermal reaction. It thus formed a $SnO_2$@C hollow sphere. After bieng annealed in $N_2$ at 700 °C, the $SnO_2$ was reduced to metallic Sn nanoparticles by the outer carbon and embedded in the carbon hollow sphere (74 wt % tin and 26 wt % carbon) as Figures 18a and 18b. It can be seen that a few tin nanoparticles are loosely wrapped in thin hollow carbon shells. The volume ratio of tin to the void is about 1: 3. Wan et al. used the as-obtained rattle-structured TNHCs as anode materials to characterize its LIB performance. Figure 18c shows the cyclic voltammograms of TNHCs that accord with the bare Sn. The cycling performance of the TNHCs is shown in Figure 18d. The as-assembled LIB has a specific capacity higher than 800 mA h $g^{-1}$ in the initial 10 cycles, and higher than 550 mA h $g^{-1}$ even after the 100th cycle, which is much higher than the graphite materials commonly used. This performance is mainly a result of the novel rattle structure of the TNHCs. First, the ample inner void of the hollow carbon shell accommodates the volume change of tin. Second, the carbon shell effectively prevents aggregation of the tin nanoparticles. Third, the high tin content provides a high specific capacity. It thereby proves that rattle-structured electrode materials are of unique advantages for future high-performance LIBs.

### 4.4. Microreactors

The abundant multiple inner void spaces of multilevel interior-structured micro/nanomaterials provide good opportunities for encapsulating several functional materials into the interior compartments. They can serve as suitable candidates for microscopically confined chemical reactions, i.e., microreactors.[37,45] Kreft and co-workers have fabricated novel shell-in-shell capsules by the layer-by-layer (LbL) self-assembly of polyelectrolytes in which two different biomolecules could be inhibited in two concentric compartments, respectively.[45] First, they used coprecipitation methods to prepare calcium carbonate microspheres in which biomacromolecule magnetite nanoparticles are loaded. The addition of magnetite nanoparticles facilitated the subsequent separation and purification process. The composite $CaCO_3$ spheres served as templates on which several layers of polystyrene sulfonate (PSS) and polyallylamine hydrochloride (PAH) were alternatively coated to form $CaCO_3$@-polymer core–shell microspheres. Another spacer layer of $CaCO_3$ was then coated on the polymer shell and another PSS–PAH shell was assembled on the formed $CaCO_3$ again. It thus formed ball-in-ball microspheres. If the $CaCO_3$ was removed by ethylenediaminetetraacetic acid (EDTA), a kind of shell-in-shell capsule was obtained. Figures 19a and 19b show capsules in which the core and surrounding compartments are dyed with biomacromolecular fluorochrome, respectively. The $CaCO_3$ is used here for two reasons: First, the $CaCO_3$ itself is a biocompatible material that can be loaded with various biomaterials. Second, the $CaCO_3$ microspheres can be dissolved by washing with a mild solution of EDTA, which is un-like routine PS or silica colloids that need to be removed by corrosive and toxic solutions. Because the core and middle layers of the shell-in-shell capsule can be respectively doped with different substances, it can act as a microreactor for confined chemical reactions. As a demonstration, Kreft et al. prepared a bi-enzymatic reactive couple: peroxidase (POD) and glucose oxidase (GOD) were loaded into the core compartment and the surrounding compartment,

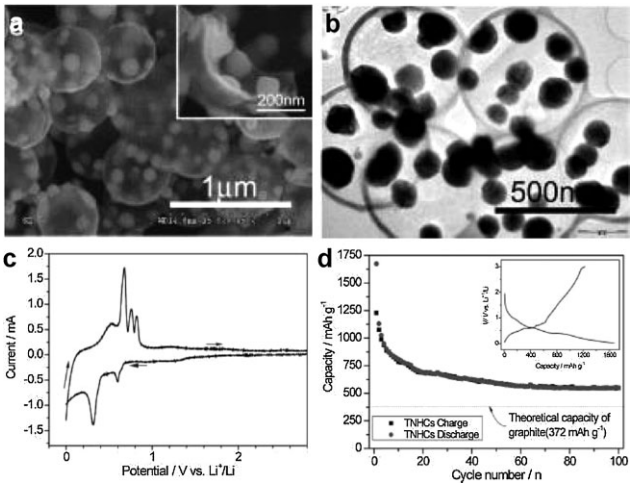


**Figure 18.** a) SEM and b) TEM images of tin nanoparticle-encapsulated elastic hollow carbon (TNHC) spheres. c) The cycle voltammograms of TNHCs, the scan speed is 0.2 mV $s^{-1}$. d) The discharge/charge capacity profiles of TNHCs in a 5 mV to 3 V (vs. $Li^+$/Li) voltage window and C/5, the inset shows the first discharge/charge profiles of TNHCs cycled at a rate of C/5. Reproduced with permission from ref. [46].

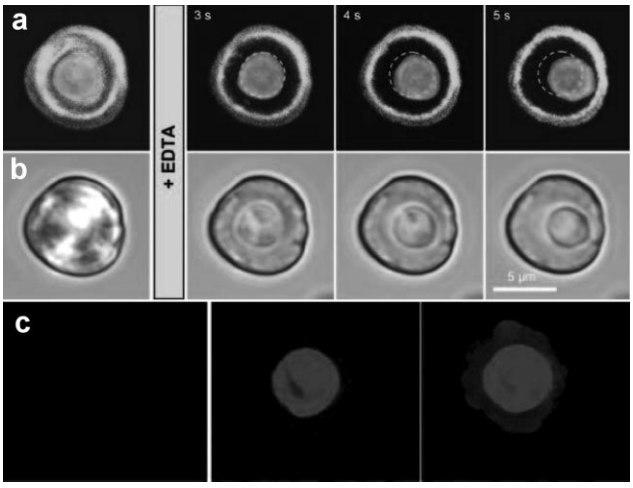


**Figure 19.** CLSM (a) and optical (b) images of the evolution of ball-in-ball particle to shell-in-shell capsule after the $CaCO_3$ is solved. The outer and inner $CaCO_3$ compartments are labeled with different fluorochromes, respectively. The core and surrounding substances are isolated all the time because of the polyelectrolyte diaphragm. c) CLSM image of a microreaction. When the glucose is added to the solution of the shell-in-shell capsule, $H_2O_2$ is generated from glucose and water by the GOD enzyme. Amplex Red is then introduced to the solution, and it is rapidly catalyzed to fluorescent resorufin by $H_2O_2$ under POD catalysis. It forms a fluorescent core and gradually diffuses to the outer shell. The capsule thus experiences a non-fluorescence, core fluorescence, and diffuse fluorescence process. Reproduced with permission from ref. [45].

respectively. The semipermeable polyelectrolytes permit small molecules to freely diffuse in and out, while large enzyme molecules cannot. After the glucose was added to the shell-in-shell capsules, the $H_2O$ would be oxidized to $H_2O_2$ in the surrounding compartment where the GOD catalyst existed. The generated $H_2O_2$ diffused to both the outer solution and core capsule. If Amplex Red is introduced into the solution at this time, it will be oxidized to fluorescent resorufin under POD catalytic action that has been previously confined to the core capsule. It thus generated fluorescence in the core capsule immediately. Because the small resorufin molecules could also penetrate out from semipermeable polyelectrolytes film, the outer capsule would also gradually appear fluorescent. This process is shown in Figure 19c. Thus, a microscopically confined chemical reaction is successfully completed. It is believed that rattle-structured materials, multishell materials, and multichamber materials are all good microreactive candidates since they have similar characteristics of confined inner contents and suitable inner spaces.

### 4.5. Biomedicines

The tunable interior structures and compositions of various multilevel-structured micro/nanomaterials make them suitable to be applied in biomedical areas, such as drug delivery[90] and therapy. Very recently, Xu and co-workers have demonstrated that FePt@$Fe_2O_3$ rattle-structured nanoparticles can be used as magnetic resonance imaging (MRI) contrast and anticancer agents simultaneously.[96] The FePt@$Fe_2O_3$ nanoparticles were synthesized by a Kirkendall hollowing mechanism. The properties of the rattle-structured nanocomposites result from the ingenious integration of two kinds of functional materials. The FePt core possessed high cytotoxicity that showed an ultralow $IC_{50}$ value. This was a result of the slow oxidation and release of FePt. At the same time, the magnetic $Fe_2O_3$ shell exhibited a stronger MR contrast enhancement effect than commercial MRI contrast agents. Such a design may guide researchers to produce many other multifunctional micro/nanomaterials.

## 5. Conclusions and Outlook

In this Review, we have summarized and cataloged some newly emerging 0D and 1D hollow micro/nanomaterials with multilevel interior structures. The representative synthetic methodology, structural related properties, and some applications of these novel microscopic materials are presented. These multilevel interior-structured materials have attracted considerable attention in a short period of time not only because of their amazingly complicated micro/nanostructures, but also their outstanding properties and broad potential applications. A number of remarkable features of these materials include: 1) abundant and tunable multilevel interior structures, 2) flexible chemical compositions, 3) huge specific area, and 4) multiphase anisotropic interfaces. Most of these properties are desired pursuits of scientists. However, it should be pointed out that the investigations in this field are still in a take-off stage. Owing to their small size and structural complexity, there are not yet versatile methodologies to generate these complex structured microscopic materials. Some synthetic strategies rely on the experiences of researchers, and a few achievements are probably windfalls in accidental cases. Every method has inherent merits and disadvantages. It thereby leaves a great deal of challenges and opportunities to scientists in many discipline domains. For example, the most commonly used template method shows overwhelming feasibility to generate most kinds of complicated structures with good structural controllability. At the same time, it possesses the broadest applicability for almost all material systems including organics, inorganics, and hybrids. Nonetheless, these approaches also have a number of obvious drawbacks. First and foremost, this method inevitably needs a troublesome multistep procedure even for the simplest hollow object. Each step needs to be operated very carefully. The fabrication of multilevel interior-structured materials further increases the practical difficulty from template preparation to subsequent coating process. The utilization and removal of a template will impart impurities to the products, which is unfavorable for high quality products. These shortcomings largely limit its large-scale production and applications. As a comparison, some self-organization methods have attracted considerable attention because of their structural construction by a simple one-pot or one-step preparation concept. For inorganics, it mainly relies on a few methods such as the Ostwald ripening, Kirkendall effect, and some others. Unlike polycrystalline or even non-crystalline materials obtained by template methods, the products of these crystallography methods possess relatively high purity. For organic molecules, self-

assembly exhibits an extraordinary capability to form various complex structures. However, these methods are often limited to specific material systems that lack universal applicability to date. The structures of the products are usually hard to predict. Although the self-assembly process itself is often a rapid process for organic molecules in most cases, the design and synthesis of the desired molecules with complex multiple functional groups is a challenge. A versatile multifluidic compound-jet electrohydrodynamic technique has exhibited excellent controllability for 0D and 1D micro/nanomaterials with programmable interior structures. This technique is suitable for a wide range of material systems including polymers, hybrids, and inorganics. It is therefore promising to become another powerful approach in addition to the widely used template route and self-assembly method. But this method also has a number of limitations such as the requirement for a polymer additive, poor crystallization for inorganics, and suitable conductivity of work solutions. Still other unconventional approaches possess individual advantages and limitations. Therefore, the universality, simplicity, quality, and quantity cannot, at least, be compared at present. How to pre-design and precisely control the desired inner structures still needs to be further explored. Further investigations in this field should be primarily concentrated on the comprehension of the formation mechanism of these complex interior structures because it is favorable to establish more effective and more economical methodological approaches for mass production. Although we have presented some recent works concerning the multilevel interior-structured micro/nanomaterials, we would rather regard this Review as an opening remark than draw conclusions since this field is so attractive and promising. We believe these multilevel interior-structured micro/nanomaterials are of tremendous potential in energy, environmental protection, bioengineering, and many other important domains.

## *Acknowledgements*

The authors acknowledge the financial support by NSFC (G.20801057, G.20774101), MoST Program (2007AA03Z327), 973 Program (2009CB930404, 2007CB936403), and the Chinese Academy of Sciences.

Received: December 10, 2008
Published online:

[1] C. Burda, X. B. Chen, R. Narayanan, M. A. El-Sayed, *Chem. Rev.* **2005**, *105*, 1025.
[2] G. Hodes, *Adv. Mater.* **2007**, *19*, 639.
[3] G. M. Whitesides, *Small* **2005**, *1*, 172.
[4] Y. N. Xia, P. D. Yang, Y. G. Sun, Y. Y. Wu, B. Mayers, B. Gates, Y. D. Yin, F. Kim, Y. Q. Yan, *Adv. Mater.* **2003**, *15*, 353.
[5] X. Wang, Y. D. Li, *Chem. Commun.* **2007**, 2901.
[6] K. Byrappa, T. Adschiri, *Prog. Cryst. Growth Charact.* **2007**, *53*, 117.
[7] E. C. Scher, L. Manna, A. P. Alivisatos, *Phil. Trans, R. Soc. Lond. A* **2003**, *361*, 241.
[8] C. N. R. Rao, F. L. Deepak, G. Gundiah, A. Govindaraj, *Prog. Solid State Chem.* **2003**, *31*, 5.
[9] J. Park, J. Joo, S. G. Kwon, Y. Jang, T. Hyeon, *Angew. Chem. Int. Ed.* **2007**, *46*, 4630.
[10] X. Wang, Q. Peng, Y. D. Li, *Acc. Chem. Res.* **2007**, *40*, 635.
[11] A. R. Tao, S. Habas, P. D. Yang, *Small* **2008**, *4*, 310.
[12] A. Zabet-Khosousi, A. A. Dhirani, *Chem. Rev.* **2008**, *108*, 4072.
[13] F. Caruso, R. A. Caruso, H. Mohwald, *Science* **1998**, *282*, 1111.
[14] J. T. Hu, T. W. Odom, C. M. Lieber, *Acc. Chem. Res.* **1999**, *32*, 435.
[15] D. T. Bong, T. D. Clark, J. R. Granja, M. R. Ghadiri, *Angew. Chem. Int. Ed.* **2001**, *40*, 988.
[16] J. Bernholc, D. Brenner, M. B. Nardelli, V. Meunier, C. Roland, *Annu. Rev. Mater. Res.* **2002**, *32*, 347.
[17] G. R. Patzke, F. Krumeich, R. Nesper, *Angew. Chem. Int. Ed.* **2002**, *41*, 2446.
[18] Y. G. Sun, B. Mayers, Y. N. Xia, *Adv. Mater.* **2003**, *15*, 641.
[19] M. Law, J. Goldberger, P. D. Yang, *Annu. Rev. Mater. Res.* **2004**, *34*, 83.
[20] G. Sukhorukov, A. Fery, H. Mohwald, *Prog. Polym. Sci* **2005**, *30*, 885.
[21] R. Tenne, C. N. R. Rao, *Philos. Trans. R. Soc. London Ser. A* **2004**, *362*, 2099.
[22] R. Tenne, *Nat. Nano.* **2006**, *1*, 103.
[23] S. Kuchibhatla, A. S. Karakoti, D. Bera, S. Seal, *Prog. Mater Sci.* **2007**, *52*, 699.
[24] J. Aizenberg, J. C. Weaver, M. S. Thanawala, V. C. Sundar, D. E. Morse, P. Fratzl, *Science* **2005**, *309*, 275.
[25] P. Fratzl, *J. R. Soc. Interface* **2007**, *4*, 637.
[26] P. Fratzl, R. Weinkamer, *Prog. Mater Sci.* **2007**, *52*, 1263.
[27] V. Salgueirino-Maceira, M. A. Correa-Duarte, *Adv. Mater.* **2007**, *19*, 4131.
[28] L. A. A. Xiong Wen Lou, Zichao Yang, *Adv. Mater.* **2008**, *20*, 3987.
[29] X. Chen, M. Knez, A. Berger, K. Nielsch, U. Gosele, M. Steinhart, *Angew. Chem. Int. Ed.* **2007**, *46*, 6829.
[30] M. Yang, J. Ma, C. L. Zhang, Z. Z. Yang, Y. F. Lu, *Angew. Chem. Int. Ed.* **2005**, *44*, 6727.
[31] H. C. Zeng, *J. Mater. Chem.* **2006**, *16*, 649.
[32] H. J. Fan, U. Gosele, M. Zacharias, *Small* **2007**, *3*, 1660.
[33] Y. Wang, A. S. Angelatos, F. Caruso, *Chem. Mater.* **2008**, *20*, 848.
[34] Y. D. Yin, R. M. Rioux, C. K. Erdonmez, S. Hughes, G. A. Somorjai, A. P. Alivisatos, *Science* **2004**, *304*, 711.
[35] X. W. Lou, C. L. Yuan, L. A. Archer, *Adv. Mater.* **2007**, *19*, 3328.
[36] A. Stein, F. Li, N. R. Denny, *Chem. Mater.* **2008**, *20*, 649.
[37] O. Kreft, A. G. Skirtach, G. B. Sukhorukov, H. Mohwald, *Adv. Mater.* **2007**, *19*, 3142.
[38] S. Okushima, T. Nisisako, T. Torii, T. Higuchi, *Langmuir* **2004**, *20*, 9905.
[39] Y. Zhao, X. Y. Cao, L. Jiang, *J. Am. Chem. Soc.* **2007**, *129*, 764.
[40] Y. G. Sun, Y. N. Xia, *Adv. Mater.* **2004**, *16*, 264.
[41] D. Y. Yan, Y. F. Zhou, J. Hou, *Science* **2004**, *303*, 65.
[42] Y. Qin, L. F. Liu, R. B. Yang, U. Gosele, M. Knez, *Nano Lett.* **2008**, *8*, 3221.
[43] H. G. Zhang, Q. S. Zhu, Y. Zhang, Y. Wang, L. Zhao, B. Yu, *Adv. Funct. Mater.* **2007**, *17*, 2766.
[44] P. M. Arnal, M. Comotti, F. Schuth, *Angew. Chem. Int. Ed.* **2006**, *45*, 8224.
[45] O. Kreft, M. Prevot, H. Mohwald, G. B. Sukhorukov, *Angew. Chem. Int. Ed.* **2007**, *46*, 5605.
[46] W. M. Zhang, J. S. Hu, Y. G. Guo, S. F. Zheng, L. S. Zhong, W. G. Song, L. J. Wan, *Adv. Mater.* **2008**, *20*, 1160.
[47] S. Iijima, *Nature* **1991**, *354*, 56.
[48] R. H. Baughman, A. A. Zakhidov, W. A. de Heer, *Science* **2002**, *297*, 787.
[49] A. Corma, *Chem. Rev.* **1997**, *97*, 2373.
[50] M. E. Davis, *Nature* **2002**, *417*, 813.
[51] Z. P. Zhu, D. S. Su, G. Weinberg, R. E. Jentoft, R. Schlogl, *Small* **2005**, *1*, 107.
[52] Y. Wan, D. Y. Zhao, *Chem. Rev.* **2007**, *107*, 2821.
[53] Y. Wan, H. F. Yang, D. Y. Zhao, *Acc. Chem. Res.* **2006**, *39*, 423.
[54] J. H. Yu, R. R. Xu, *Acc. Chem. Res.* **2003**, *36*, 481.
[55] A. K. Cheetham, G. Ferey, T. Loiseau, *Angew. Chem. Int. Ed.* **1999**, *38*, 3268.
[56] E. Hosono, S. Fujihara, H. Lmai, I. Honma, I. Masaki, H. S. Zhou, *ACS Nano* **2007**, *1*, 273.
[57] Y. Zhu, D. Hu, M. X. Wan, L. Jiang, Y. Wei, *Adv. Mater.* **2007**, *19*, 2092.
[58] Z. Q. Li, Y. Ding, Y. J. Xiong, Q. Yang, Y. Xie, *Chem. Eur. J.* **2004**, *10*, 5823.
[59] L. Jiang, X. J. Feng, J. Zhai, M. H. Jin, Y. L. Song, D. B. Zhu, *J. Nanosci. Nanotechnol.* **2006**, *6*, 1830.
[60] L. Manna, E. C. Scher, A. P. Alivisatos, *J. Am. Chem. Soc.* **2000**, *122*, 12 700.

[61] R. Ostermann, D. Li, Y. D. Yin, J. T. McCann, Y. N. Xia, *Nano Lett.* **2006**, *6*, 1297.
[62] Y. Q. Zhu, W. K. Hsu, W. Z. Zhou, M. Terrones, H. W. Kroto, D. R. M. Walton, *Chem. Phys. Lett.* **2001**, *347*, 337.
[63] Z. R. Dai, Z. W. Pan, Z. L. Wang, *Adv. Funct. Mater.* **2003**, *13*, 9.
[64] C. H. Sun, N. X. Wang, S. Y. Zhou, X. J. Hu, P. Chen, *Chem. Commun.* **2008**, 3293.
[65] N. X. Wang, C. H. Sun, Y. Zhao, S. Y. Zhou, P. Chen, L. Jiang, *J. Mater. Chem.* **2008**, *18*, 3909.
[66] K. A. Dick, K. Deppert, M. W. Larsson, T. Martensson, W. Seifert, L. R. Wallenberg, L. Samuelson, *Nat. Mater.* **2004**, *3*, 380.
[67] L. W. Yin, Y. Bando, Y. C. Zhu, M. S. Li, Y. B. Li, D. Golberg, *Adv. Mater.* **2005**, *17*, 110.
[68] J. Zhou, Y. Ding, S. Z. Deng, L. Gong, N. S. Xu, Z. L. Wang, *Adv. Mater.* **2005**, *17*, 2107.
[69] J. Zhou, S. Z. Deng, J. Chen, J. C. She, N. X. Xu, *Chem. Phys. Lett.* **2002**, *365*, 505.
[70] J. Y. Lao, J. Y. Huang, D. Z. Wang, Z. F. Ren, *J. Mater. Chem.* **2004**, *14*, 770.
[71] J. Wan, A. Bick, M. Sullivan, H. A. Stone, *Adv. Mater.* **2008**, *20*, 3314.
[72] T. Shiomi, T. Tsunoda, A. Kawai, F. Mizukami, K. Sakaguchi, *Chem. Commun.* **2007**, 4404.
[73] Y. S. Cho, G. R. Yi, S. H. Kim, S. J. Jeon, M. T. Elsesser, H. K. Yu, S. M. Yang, D. J. Pine, *Chem. Mater.* **2007**, *19*, 3183.
[74] X. D. He, X. W. Ge, H. R. Liu, M. Z. Wang, Z. C. Zhang, *Chem. Mater.* **2005**, *17*, 5891.
[75] E. Kamio, S. Yonemura, T. Ono, H. Yoshizawa, *Langmuir* **2008**, *24*, 13 287.
[76] S. Yang, H. R. Liu, Z. C. Zhang, *Langmuir* **2008**, *24*, 10 395.
[77] Q. Wei, W. Wei, R. Tian, L. Y. Wang, Z. G. Su, G. H. Ma, *J. Colloid Interface Sci.* **2008**, *323*, 267.
[78] G. H. Ma, H. Sone, S. Omi, *Macromolecules* **2004**, *37*, 2954.
[79] W. Wei, L. Y. Wang, L. Yuan, Q. Wei, X. D. Yang, Z. G. Su, G. H. Ma, *Adv. Funct. Mater.* **2007**, *17*, 3153.
[80] R. W. Wang, Y. Zhang, G. G. Ma, Z. G. Su, *J. Appl. Polym. Sci.* **2006**, *102*, 5018.
[81] Q. Z. Zhou, L. Y. Wang, G. H. Ma, Z. G. Su, *J. Colloid Interface Sci.* **2007**, *311*, 118.
[82] W. Q. Zhou, T. Y. Gu, Z. G. Su, G. H. Ma, *Polymer* **2007**, *48*, 1981.
[83] L. Jiang, Y. Zhao, J. Zhai, *Angew. Chem. Int. Ed.* **2004**, *43*, 4338.
[84] Y. Zhao, J. Zhai, S. X. Tan, L. F. Wang, L. Jiang, D. B. Zhu, *Nanotechnology* **2006**, *17*, 2090.
[85] F. Iskandar, A. B. D. Nandiyanto, K. M. Yun, C. J. Hogan, K. Okuyama, P. Biswas, *Adv. Mater.* **2007**, *19*, 1408.
[86] D. M. Kuncicky, K. Bose, K. D. Costa, O. D. Velev, *Chem. Mater.* **2007**, *19*, 141.
[87] H. Y. Li, H. Q. Wang, A. H. Chen, B. Meng, X. Y. Li, *J. Mater. Chem.* **2005**, *15*, 2551.
[88] F. Iskandar, Mikrajuddin, K. Okuyama, *Nano Lett.* **2002**, *2*, 389.
[89] Y. Y. Mai, Y. F. Zhou, D. Y. Yan, *Small* **2007**, *3*, 1170.
[90] W. R. Zhao, H. R. Chen, Y. S. Li, L. Li, M. D. Lang, J. L. Shi, *Adv. Funct. Mater.* **2008**, *18*, 2780.
[91] H. J. Hah, J. I. Um, S. H. Han, S. M. Koo, *Chem. Commun.* **2004**, 1012.
[92] M. Kim, K. Sohn, H. Bin Na, T. Hyeon, *Nano Lett.* **2002**, *2*, 1383.
[93] J. H. Yang, L. H. Lu, H. S. Wang, H. J. Zhang, *Scripta Mater.* **2006**, *54*, 159.
[94] J. Lee, J. C. Park, H. Song, *Adv. Mater.* **2008**, *20*, 1523.
[95] M. Chen, Y. N. Kim, H. M. Lee, C. Li, S. O. Cho, *J. Phys. Chem. C* **2008**, *112*, 8870.
[96] J. H. Gao, G. L. Liang, J. S. Cheung, Y. Pan, Y. Kuang, F. Zhao, B. Zhang, X. X. Zhang, E. X. Wu, B. Xu, *J. Am. Chem. Soc.* **2008**, *130*, 11 828.
[97] S. Ikeda, Y. Ikoma, H. Kobayashi, T. Harada, T. Torimoto, B. Ohtani, M. Matsumura, *Chem. Commun.* **2007**, 3753.
[98] X. W. Lou, L. A. Archer, *Adv. Mater.* **2008**, *20*, 1853.
[99] X. W. Lou, Y. Wang, C. L. Yuan, J. Y. Lee, L. A. Archer, *Adv. Mater.* **2006**, *18*, 2325.
[100] W. S. Choi, H. Y. Koo, D. Y. Kim, *Adv. Mater.* **2007**, *19*, 451.
[101] J. Y. Kim, S. B. Yoon, J. S. Yu, *Chem. Commun.* **2003**, 790.
[102] J. Lee, J. C. Park, J. U. Bang, H. Song, *Chem. Mater.* **2008**, *20*, 5839.
[103] N. Ren, B. Wang, Y. H. Yang, Y. H. Zhang, W. L. Yang, Y. H. Yue, Z. Gao, Y. Tang, *Chem. Mater.* **2005**, *17*, 2582.
[104] K. Kamata, Y. Lu, Y. N. Xia, *J. Am. Chem. Soc.* **2003**, *125*, 2384.
[105] W. S. Choi, H. Y. Koo, D. Y. Kim, *Langmuir* **2008**, *24*, 4633.
[106] Z. Kai, X. H. Zhang, H. T. Chen, C. Xin, L. L. Zheng, J. H. Zhang, Y. Bai, *Langmuir* **2004**, *20*, 11 312.
[107] G. Y. Liu, H. F. Ji, X. L. Yang, Y. M. Wang, *Langmuir* **2008**, *24*, 1019.
[108] T. R. Zhang, J. P. Ge, Y. X. Hu, Q. Zhang, S. Aloni, Y. D. Yin, *Angew. Chem. Int. Ed.* **2008**, *47*, 5806.
[109] S. Ikeda, S. Ishino, T. Harada, N. Okamoto, T. Sakata, H. Mori, S. Kuwabata, T. Torimoto, M. Matsumura, *Angew. Chem. Int. Ed.* **2006**, *45*, 7063.
[110] Q. Zhang, T. R. Zhang, J. P. Ge, Y. D. Yin, *Nano Lett.* **2008**, *8*, 2867.
[111] X. W. Lou, C. Yuan, Q. Zhang, L. A. Archer, *Angew. Chem. Int. Ed.* **2006**, *45*, 3825.
[112] H. J. Fan, M. Knez, R. Scholz, K. Nielsch, E. Pippel, D. Hesse, M. Zacharias, U. Gosele, *Nat. Mater.* **2006**, *5*, 627.
[113] X. Liang, B. A. Xu, S. M. Kuang, X. Wang, *Adv. Mater.* **2008**, *20*, 3739.
[114] X. W. Lou, C. L. Yuan, E. Rhoades, Q. Zhang, L. A. Archer, *Adv. Funct. Mater.* **2006**, *16*, 1679.
[115] J. Li, H. C. Zeng, *J. Am. Chem. Soc.* **2007**, *129*, 15 839.
[116] B. Liu, H. C. Zeng, *Small* **2005**, *1*, 566.
[117] A. Blanco, C. Lopez, *Adv. Mater.* **2006**, *18*, 1593.
[118] M. Yang, J. Ma, Z. W. Niu, X. Dong, H. F. Xu, Z. K. Meng, Z. G. Jin, Y. F. Lu, Z. B. Hu, Z. Z. Yang, *Adv. Funct. Mater.* **2005**, *15*, 1523.
[119] X. L. Xu, S. A. Asher, *J. Am. Chem. Soc.* **2004**, *126*, 7940.
[120] J. Zhou, M. Chen, X. G. Qiao, L. M. Wu, *Langmuir* **2006**, *22*, 10 175.
[121] Z. Chen, Z. L. Wang, P. Zhan, J. H. Zhang, W. Y. Zhang, H. T. Wang, N. B. Ming, *Langmuir* **2004**, *20*, 3042.
[122] Z. F. Dai, L. Dahne, H. Mohwald, B. Tiersch, *Angew. Chem. Int. Ed.* **2002**, *41*, 4019.
[123] Z. F. Dai, H. Mohwald, B. Tiersch, L. Dahne, *Langmuir* **2002**, *18*, 9533.
[124] V. Salgueirino-Maceira, M. Spasova, M. Farle, *Adv. Funct. Mater.* **2005**, *15*, 1036.
[125] K. Kohler, G. B. Sukhorukov, *Adv. Funct. Mater.* **2007**, *17*, 2053.
[126] A. Petukhova, A. S. Paton, Z. X. Wei, I. Gourevich, S. V. Nair, H. E. Ruda, A. Shik, E. Kumacheva, *Adv. Funct. Mater.* **2008**, *18*, 1961.
[127] X. W. Lou, C. L. Yuan, L. A. Archer, *Small* **2007**, *3*, 261.
[128] H. Zhao, J. F. Chen, Y. Zhao, L. Jiang, J. W. Sun, J. Yun, *Adv. Mater.* **2008**, *20*, 3682.
[129] T. Nisisako, S. Okushima, T. Torii, *Soft Matter* **2005**, *1*, 23.
[130] L. Y. Chu, A. S. Utada, R. K. Shah, J. W. Kim, D. A. Weitz, *Angew. Chem. Int. Ed.* **2007**, *46*, 8970.
[131] H. Y. Chen, Y. Zhao, Y. L. Song, L. Jiang, *J. Am. Chem. Soc.* **2008**, *130*, 7800.
[132] M. Knez, K. Niesch, L. Niinisto, *Adv. Mater.* **2007**, *19*, 3425.
[133] A. V. Bazilevsky, K. X. Sun, A. L. Yarin, C. M. Megaridis, *Langmuir* **2007**, *23*, 7451.
[134] L. F. Liu, W. Lee, R. Scholz, E. Pippel, U. Gosele, *Angew. Chem. Int. Ed.* **2008**, *47*, 7004.
[135] C. H. Hsieh, L. J. Chou, G. R. Lin, Y. Bando, D. Golberg, *Nano Lett.* **2008**, *8*, 3081.
[136] E. Zussman, A. L. Yarin, A. V. Bazilevsky, R. Avrahami, M. Feldman, *Adv. Mater.* **2006**, *18*, 348.
[137] Z. Y. Yao, X. Zhu, C. Z. Wu, X. J. Zhang, Y. Xie, *Cryst. Growth Des.* **2007**, *7*, 1256.
[138] J. Zhang, Y. S. Hu, J. P. Tessonnier, G. Weinberg, J. Maier, R. Schlogl, D. S. Su, *Adv. Mater.* **2008**, *20*, 1450.
[139] D. H. Reneker, I. Chun, *Nanotechnology* **1996**, *7*, 216.

[140] Z. M. Huang, Y. Z. Zhang, M. Kotaki, S. Ramakrishna, *Compos. Sci. Technol.* **2003**, *63*, 2223.
[141] D. Li, Y. N. Xia, *Adv. Mater.* **2004**, *16*, 1151.
[142] D. Li, Y. N. Xia, *Nano Lett.* **2004**, *4*, 933.
[143] I. G. Loscertales, A. Barrero, I. Guerrero, R. Cortijo, M. Marquez, A. M. Ganan-Calvo, *Science* **2002**, *295*, 1695.
[144] Y. G. Sun, B. Wiley, Z. Y. Li, Y. N. Xia, *J. Am. Chem. Soc.* **2004**, *126*, 9399.
[145] C. J. Jia, L. D. Sun, Z. G. Yan, Y. C. Pang, L. P. You, C. H. Yan, *J. Phys. Chem. C* **2007**, *111*, 13 022.
[146] Y. Yamamoto, T. Fukushima, Y. Suna, N. Ishii, A. Saeki, S. Seki, S. Tagawa, M. Taniguchi, T. Kawai, T. Aida, *Science* **2006**, *314*, 1761.
[147] Y. L. Chen, B. Zhu, F. Zhang, Y. Han, Z. S. Bo, *Angew. Chem. Int. Ed.* **2008**, *47*, 6015.
[148] O. Kriha, L. L. Zhao, E. Pippel, U. Gosele, R. B. Wehrspohn, J. H. Wendorff, M. Steinhart, A. Greiner, *Adv. Funct. Mater.* **2007**, *17*, 1327.
[149] V. Luchnikov, O. Sydorenko, M. Stamm, *Adv. Mater.* **2005**, *17*, 1177.
[150] J. Xu, W. X. Zhang, Z. H. Yang, S. H. Yang, *Inorg. Chem.* **2008**, *47*, 699.
[151] S. L. Bai, J. H. Zhao, G. X. Du, J. F. Zheng, Z. P. Zhu, *Nanotechnology* **2008**, *19*, 205605.
[152] Z. B. Zhao, J. Y. Qu, J. S. Qiu, X. Z. Wang, Z. Y. Wang, *Chem. Commun.* **2006**, 594.
[153] W. Z. Xu, Z. Z. Ye, D. W. Ma, H. M. Lu, L. P. Zhu, B. H. Zhao, X. D. Yang, Z. Y. Xu, *Appl. Phys. Lett.* **2005**, *87*.
[154] J. S. Lee, G. H. Gu, H. Kim, K. S. Jeong, J. Bae, J. S. Suh, *Chem. Mater.* **2001**, *13*, 2387.
[155] X. W. Zhao, P. Jiang, W. G. Chu, S. C. Mu, D. F. Liu, L. Song, L. F. Liu, S. D. Luo, Z. X. Zhang, Y. J. Xiang, W. Y. Zhou, G. Wang, S. S. Xie, *Carbon* **2006**, *44*, 1310.
[156] B. Yameen, A. Kaltbeitzel, A. Langner, H. Duran, F. Muller, U. Gosele, O. Azzaroni, W. Knoll, *J. Am. Chem. Soc.* **2008**, *130*, 13 140.
[157] L. X. Yang, S. L. Luo, S. H. Liu, Q. Y. Cai, *J. Phys. Chem. C* **2008**, *112*, 8939.
[158] D. Y. Xia, T. C. Gamble, E. A. Mendoza, S. J. Koch, X. He, G. P. Lopez, S. R. J. Brueck, *Nano Lett.* **2008**, *8*, 1610.
[159] Y. Zhao, X. L. Sheng, J. Zhai, L. Jiang, C. H. Yang, Z. W. Sun, Y. F. Li, D. B. Zhu, *ChemPhysChem* **2007**, *8*, 856.
[160] X. W. Lou, D. Deng, J. Y. Lee, L. A. Archer, *Chem. Mater.* **2008**, *20*, 6562.
[161] H. X. Yang, J. F. Qian, Z. X. Chen, X. P. Ai, Y. L. Cao, *J. Phys. Chem. C* **2007**, *111*, 14 067.
[162] K. T. Lee, Y. S. Jung, S. M. Oh, *J. Am. Chem. Soc.* **2003**, *125*, 5652.

WILEY InterScience® DISCOVER SOMETHING GREAT

# JOURNALS



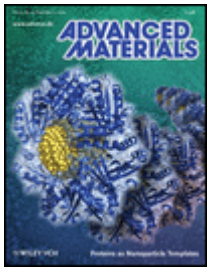

## Advanced Materials



Get Sample Copy
Recommend to Your Librarian
Save journal to My Profile
Set E-Mail Alert
Email this page
Print this page
RSS web feed (What is RSS?)

Journal Home | News | Read Cover Story | **Most Accessed** | Most Cited
Product Information | Editorial Board | For Authors | For Referees | Subscribe | Advertise | Contact | Online Submission | Article Index | Virtual Issues

ISSUE NAVIGATION Early View | Current Issue | 2009 | 2008 | 2007 | 2006 | 2005 | ALL ISSUES (1989 - 2009)

## Most accessed articles in 06/2009

- Yapei Wang, Huaping Xu, Xi Zhang
  Tuning the Amphiphilicity of Building Blocks: Controlled Self-Assembly and Disassembly for Functional Supramolecular Materials [Review Article]
  *Adv. Mater.*, DOI: 10.1002/adma.200803276 (EarlyView)
- Hongbin Wu, Guijiang Zhou, Jianhua Zou, Cheuk-Lam Ho, Wai-Yeung Wong, Wei Yang, Junbiao Peng, Yong Cao
  Efficient Polymer White-Light-Emitting Devices for Solid-State Lighting [Communication]
  *Adv. Mater.*, DOI: 10.1002/adma.200900638 (EarlyView)
- Leena Nebhani, Christopher Barner-Kowollik
  Orthogonal Transformations on Solid Substrates: Efficient Avenues to Surface Modification [Review Article]
  *Adv. Mater.*, DOI: 10.1002/adma.200900238 (EarlyView)
- Nir Tessler *, Yevgeni Preezant, Noam Rappaport, Yohai Roichman
  Charge Transport in Disordered Organic Materials and Its Relevance to Thin-Film Devices: A Tutorial Review [Review Article]
  *Adv. Mater.* , vol. 21, no. 27, pp. 2741–2761
- Ragip A. Pala, Justin White, Edward Barnard, John Liu, Mark L. Brongersma
  Design of Plasmonic Thin-Film Solar Cells with Broadband Absorption Enhancements [Communication]
  *Adv. Mater.*, DOI: 10.1002/adma.200900331 (EarlyView)
- Dong Chen , Linlin Li , Fangqiong Tang, Shuo Qi
  Facile and Scalable Synthesis of Tailored Silica “Nanorattle” Structures [Communication]
  *Adv. Mater.*, DOI: 10.1002/adma.200900599 (EarlyView)
- Jung Hak Kim, Myungeun Seo, Sang Youl Kim
  Lithographically Patterned Breath Figure of Photoresponsive Small Molecules: Dual-Patterned Honeycomb Lines from a Combination of Bottom-Up and Top-Down Lithography [Communication]
  *Adv. Mater.*, DOI: 10.1002/adma.200900868 (EarlyView)
- Stefan Mátéfi-Tempfli, Mária Mátéfi-Tempfli
  Vertically Aligned Nanowires on Flexible Silicone using a Supported Alumina Template prepared by Pulsed Anodization [Communication]
  *Adv. Mater.*, DOI: 10.1002/adma.200900344 (EarlyView)
- Leonie Barner
  Synthesis of Microspheres as Versatile Functional Scaffolds for Materials Science Applications [Research News]
  *Adv. Mater.* 2009, vol. 21, no. 24, pp. 2547–2553
- Hisashi Yamada, Tadashi Nakamura, Yuri Yamada, Kazuhisa Yano
  Colloidal-Crystal Laser Using Monodispersed Mesoporous Silica Spheres [Communication]
  *Adv. Mater.*, DOI: 10.1002/adma.200900721 (EarlyView)
- Stephanie S. Lee, Chang Su Kim, Enrique D. Gomez, Balaji Purushothaman, Michael F. Toney, Cheng Wang, Alexander Hexemer, John. E. Anthony, Yueh-Lin Loo
  Controlling Nucleation and Crystallization in Solution-Processed Organic Semiconductors for Thin-Film Transistors [Communication]
  *Adv. Mater.*, DOI: 10.1002/adma.200900705 (EarlyView)
- Yong Zhao, Lei Jiang
  Hollow Micro/Nanomaterials with Multilevel Interior Structures [Review]
  *Adv. Mater.*, DOI: 10.1002/adma.200803645 (EarlyView)